PG
Petroleum Geoscience

Research article

https://doi.org/10.1144/petgeo2021-090 | Vol. 28 | 2022 | petgeo2021-090

New insights into the structure, geology and hydrocarbon prospectivity along the central-northern Corona Ridge, Faroe–Shetland Basin

Lucinda K. Layfield[1]*, Nick Schofield[1], David W. Jolley[1], Simon P. Holford[2], Tudor-Remus Volintir[3], Ben A. Kilhams[1], David K. Muirhead[1] and Helen Cromie[4]

[1] Department of Geology and Geophysics, University of Aberdeen, King's College, Aberdeen AB24 3EU, UK
[2] Australian School of Petroleum and Energy Resources, University of Adelaide, Adelaide, SA 5005, Australia
[3] Schlumberger, Bulevardul Timişoara 15, Bucureşti 061344, Romania
[4] TotalEnergies Upstream Danmark A/S, Amerika Plads 29, 2100 Copenhagen, Denmark

LKL, 0000-0002-5693-4959; DWJ, 0000-0003-0909-2952; SPH, 0000-0002-4524-8822; BAK, 0000-0002-4444-6800; DKM, 0000-0003-2065-6042

Present address: HC, Ørsted Wind Power, Nesa Allé 1, 2820 Gentofte, Denmark

* Correspondence: l.layfield.18@abdn.ac.uk

Abstract: The Faroe–Shetland Basin (FSB) is one of the only significant exploration frontiers remaining on the UK Continental Shelf. Over half of the basin's discovered reserves and resources lie along two intra-basinal highs, the Corona Ridge and the Rona Ridge. In contrast to the Rona Ridge, the central-northern Corona Ridge has received much less attention. To reveal new insights into the geology, structural configuration and hydrocarbon prospectivity of the central-northern Corona Ridge, we analyse 3D seismic data and data from the exploration wells 213/23-1 (Eriboll), 214/21a-2 (South Uist) and 213/25c-1V (North Uist). This study extends the Colsay T40–T45 sub- and intra-basaltic play concept from the Rosebank Field NE along the Corona Ridge, at least into well 213/23-1. Analysis also suggests that no Triassic strata are present within well 213/23-1, challenging the previous understanding of Triassic distribution within the central FSB. Our findings show that the central-northern Corona Ridge is structurally complex, comprising a series of discrete basement-bounding faults, downflank fault terraces and faults that are oblique to the dominant NE–SW-striking structural fabric of the FSB.

Received 4 November 2021; **revised** 6 June 2022; **accepted** 14 July 2022

The Faroe–Shetland Basin (FSB), located west of the Shetland Isles on the NE Atlantic continental margin (Fig. 1), is one of the only remaining significant exploration frontiers on the UK Continental Shelf (UKCS), and will also arguably be one of the most important areas to contribute to indigenous oil and gas supply in the next 40 years (Austin *et al.* 2014; Ellis and Stoker 2014). As of September 2021, the region is estimated to hold *c*. 3.7 Bboe (billion barrels of oil equivalent) of discovered reserves and contingent resources, around 30% of the UK's total (2P and 2C: North Sea Transition Authority 2019). In 2019, the UKs North Sea Transition Authority (NSTA) estimated mean yet-to-find resources of 5.8 Bboe within the West of Shetland region, totalling 38% of the estimated yet-to-find resources across the entire UKCS (encompassing lead, prospect and play-level prospective resources: North Sea Transition Authority 2019).

Particularly prospective areas of the FSB include intra-basinal highs; in total, over half of the discovered reserves and contingent resources in the basin are situated on the Corona Ridge and the Rona Ridge (Fig. 1) (Austin *et al.* 2014; Scotchman *et al.* 2016; North Sea Transition Authority 2019). Significant discoveries, some now developed and in production, have been made along the Rona Ridge (Fig. 1b) within early Cretaceous shallow to marginal-marine (Victory Field: Goodchild *et al.* 1999) and marine (Edradour Field: Clark *et al.* 2020) sandstones, fractured Precambrian crystalline basement rocks (e.g. Clair Ridge: Robertson *et al.* 2020), and Devonian-age siliciclastic rocks of the Lower Clair Group (Clair Field: Robertson *et al.* 2020) (Fig. 2).

Exploration focused along the Corona Ridge has provided encouraging results (e.g. Rosebank and Cambo fields, and Lochnagar and Blackrock discoveries: Fig. 1b). However, in contrast to the Rona Ridge (on which the Clair and Lancaster fields are developed), as of August 2022, none of the discoveries made along the Corona Ridge have been sanctioned for development. The 300 MMboe (million barrels of oil equivalent) (recoverable) Rosebank Field, reservoired within the upper Paleocene–lower Eocene-aged fluvial–deltaic intra- and sub-basaltic Colsay Member (T40–T45) sandstone units, is currently awaiting a final investment decision (FID: estimated in 2022), 18 years since its discovery in 2004 (Siccar Point Energy 2020*a*). Planned sanction of the Cambo Field (30 km SW of Rosebank) was expected within 2022, with first oil projected for 2025, which will be 23 years after the discovery of 800 MMboe (in place) within Hildasay Member (T45) sandstones in 2002 (Siccar Point Energy 2020*a*, *b*).

The Cambo and Rosebank discoveries currently represent the largest undeveloped accumulation in the UKCS (as of September 2022), totalling *c.* 700 MMboe of recoverable resources (Austin *et al.* 2014; Siccar Point Energy 2020*a*). In addition to Cambo and Rosebank, hydrocarbon shows and discoveries have been encountered within multiple stratigraphic intervals along the Corona Ridge, including the Carboniferous North Uist (well 213/25c-1V), Jurassic Lochnagar (well 213/27-1Z), Paleocene Bunnehaven (well 214/09-1), Paleocene–Eocene Blackrock (well 204/05b-2) and Eocene Tobermory (well 214/04-1) discoveries (Figs 1 and 2).

Whilst hydrocarbon shows and discoveries prove a working petroleum system is present both along the Corona Ridge and within the basins bound by the Corona Ridge, as highlighted by Scotchman *et al.* (2006, 2016), Mark *et al.* (2018*a*, *b*) and Gardiner *et al.* (2019), many aspects of the region's petroleum geology are still not fully understood – as emphasized by recent disappointing results of wells drilled along the Corona Ridge (Lochnagar appraisal, well

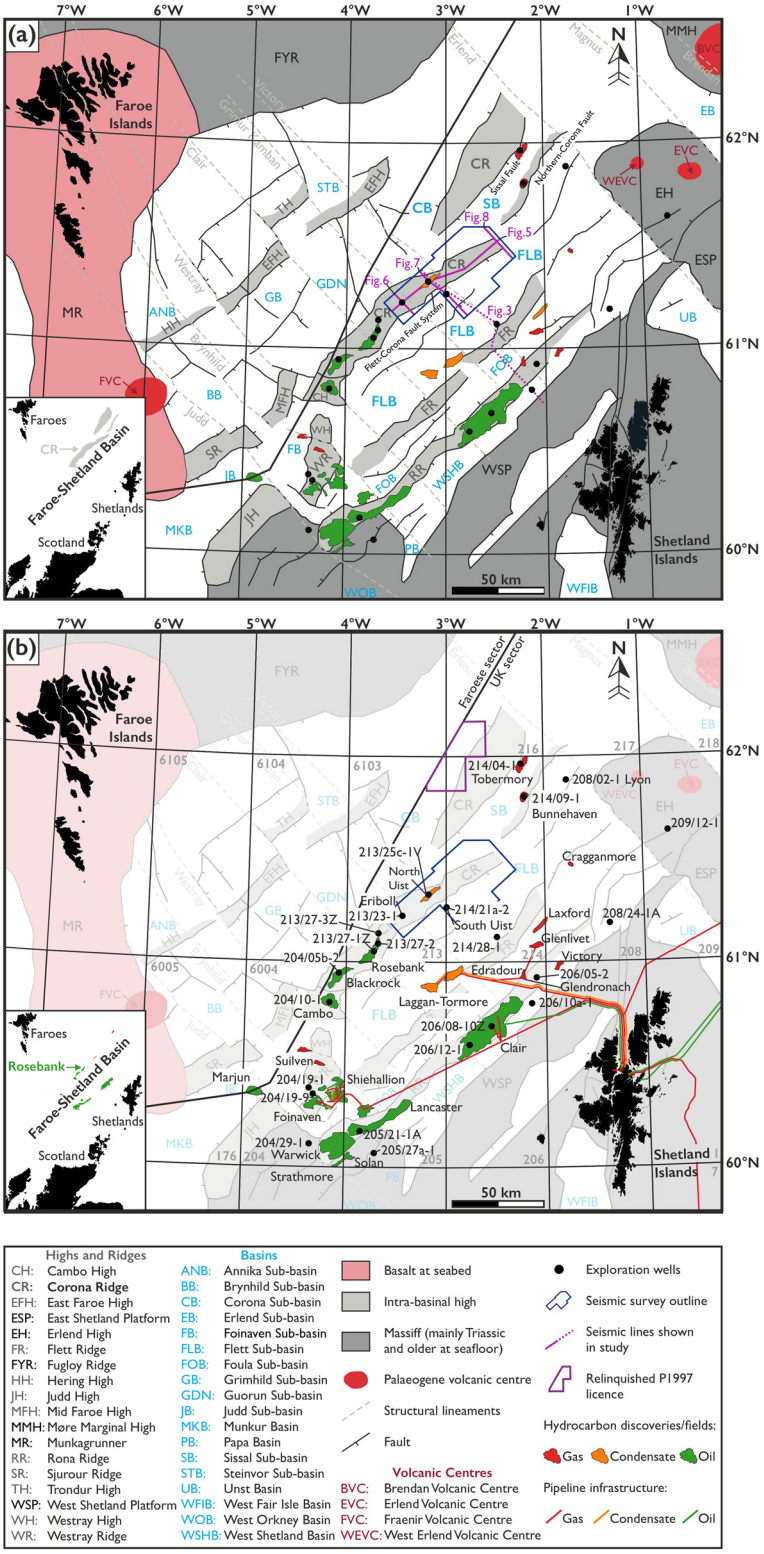

Fig. 1. (**a**) Map of the Faroe–Shetland Basin highlighting the main structural elements and study area. Note the presence of the Cambo, Rosebank and Clair fields, and other discoveries along the Corona and Rona intra-basinal highs (light grey). The map also shows the coverage outline of the Corona 3D seismic survey and the location of seismic lines shown in this study. (**b**) Map (a) overlain with key wells and fields discussed with pipeline infrastructure within the Faroe–Shetland Basin. Figure adapted from Ritchie *et al.* (2011) and Mark *et al.* (2018*b*) with structural lineaments (also referred to as transfer zones) and intra-basinal highs modified from Ellis *et al.* (2009) and Hardman *et al.* (2018).

213/27-3Z drilled in 2009: Fig. 1b) and *c.* 15 km from the northern Corona Ridge (Lyon prospect, well 208/02-1 drilled in 2019: Fig. 1b) (see Siccar Point Energy 2020*c*, 2020*d*).

Within the last two decades, exploration focus and success along the Corona Ridge has been largely confined to the post-rift Paleocene–Eocene-aged reservoirs around the Rosebank Field, located along the southern part of the Corona Ridge (Smallwood and Kirk 2005; Loizou 2014). Consequently, published literature of the structure, evolution and geology of the central-northern Corona Ridge is sparse, especially when compared with the prolific Rona Ridge. This is largely the result of basaltic lava cover that extends from the Faroe Islands into the FSB over much of the Corona Ridge, resulting in challenging sub-basaltic seismic imaging (Schofield and Jolley 2013). Published research has largely overlooked the possible distribution of intra- and sub-basaltic Paleocene–Eocene-aged (sequence T40–T45) reservoirs NE of the Rosebank Field and older pre-rift (Devonian–Jurassic) strata present along the central-northern Corona Ridge. Many of the exploration wells drilled along the Corona Ridge were drilled within the late 1990s and early 2000s (e.g. 213/23-1, 214/04-1 and 214/09-1: Fig. 1b), prior to key advancements in the understanding of the evolution and lithostratigraphy of the FSB and specifically the Corona Ridge.

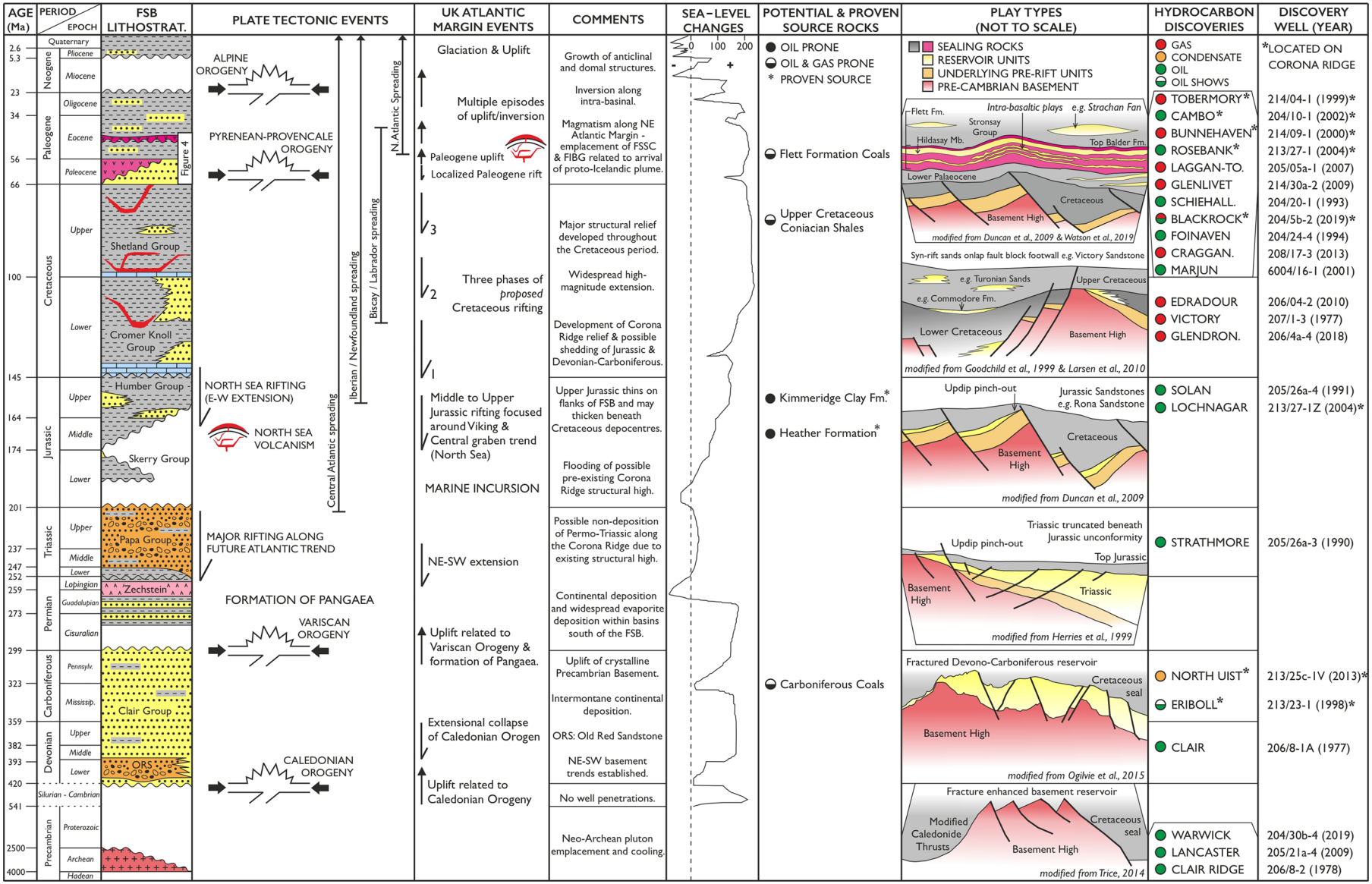

Fig. 2. Faroe–Shetland Basin tectonic history and lithostratigraphy with various aspects of the basin's petroleum system and associated discoveries. Numerical ages and chronostratigraphy are taken from the International Chronostratigraphic Chart 2020 (Cohen *et al.* 2013). The figure and lithostratigraphy are modified from Scotchman *et al.* (2006) and stratigraphic units (groups) from Ritchie *et al.* (2011). Plate tectonic events and UK Atlantic margin events are based on Scotchman *et al.* (2006), Ritchie *et al.* (2011) and Schöpfer and Hinsch (2019). The sea-level curve is modified from Haq *et al.* (1987). Potential and proven source rocks are from both Scotchman *et al.* (2006) and Quinn *et al.* (2011). Play types are modified from numerous authors individually cited (Goodchild *et al.* 1999; Herries *et al.* 1999; Duncan *et al.* 2009; Larsen *et al.* 2010; Trice 2014; Ogilvie *et al.* 2015; Watson *et al.* 2019). Note: wells and discoveries located along the Corona Ridge are shown with an asterisk (*); Eriboll (213/23-1) contained only oil shows and is added for context.

At the time of publication, over 100 MMboe of condensate and 656 bcf (billion cubic feet) of stranded gas lies undeveloped along the central-northern Corona Ridge, currently viewed as uneconomic for development without a substantial discovery nearby to warrant the development of gas infrastructure as a tieback option (P_{50} post-drill in-place volume estimates: Tobermory 464 bcf, ExxonMobil 2000; Bunnehaven 192 bcf, ExxonMobil 2001; North Uist 104 MMboe, CNOOC Ltd 2017).

The objective of this paper is to provide new insights into the structural configuration, geology and hydrocarbon prospectivity of the central-northern Corona Ridge, which lies within an area in need of a substantial discovery, through the interpretation of 3D seismic data integrated with post-well analysis of three exploration wells (213/23-1 (Eriboll), 214/21a-2 (South Uist) and 213/25c-1V (North Uist): Fig. 1b).

By analysing well data, we interpret that no Triassic-age strata are present within well 213/23-1 (Eriboll) and possibly the central FSB entirely, challenging the previous understanding of the distribution of Triassic strata within the centre of the basin (Quinn and Ziska 2011; Stoker *et al.* 2014, 2017*b*). We also extend the Colsay Member intra- and sub-basaltic play concept NE along the Corona Ridge from the Rosebank Field into well 213/23-1 (Eriboll). Our findings also suggest that the central-northern Corona Ridge is structurally complex, with evidence of north–south- and NNW–SSE-striking normal faults that are oblique to the basinal NE–SW-striking structural trends.

Geological history

The Faroe–Shetland Basin (FSB) is located between the Shetland and Faroe Islands on the NE Atlantic passive continental margin of NW Europe (Fig. 1), bound by the Wyville–Thomson Ridge (UKCS) to the SW and the Møre Marginal High (Norwegian Continental Shelf) to the NE (Ziska and Varming 2008; Ritchie *et al.* 2011). The FSB is up to 400 km long and 250 km wide, and constitutes a series of smaller rift-related sub-basins that formed throughout several main phases of extension between the early Cretaceous and the early Cenozoic (Ritchie *et al.* 2011). The sub-basins are separated by NE–SW-trending, intra-basinal structural highs comprising Precambrian crystalline rock (Figs 1 and 3) that are commonly unconformably capped by incomplete occurrences of pre-rift Paleozoic–Jurassic sedimentary rocks (Lamers and Carmichael 1999; Sørensen 2003; Peacock and Banks 2020).

Precambrian crystalline basement, observed onshore Scotland as the Lewisian Gneiss Complex, is understood to have formed after Neoarchean pluton emplacement and cooling between 2800 and 2700 Ma (Bonter and Trice 2019; Holdsworth *et al.* 2019; Peacock and Banks 2020). Offshore within the FSB, basement rocks are generally considered to be equivalent to the Lewisian Gneiss Complex (Holdsworth *et al.* 2019), and have been cored and dated to the Neorchean (Ritchie *et al.* 2011). Wells that have penetrated crystalline basement within the FSB have typically encountered Neoarchean quartzofeldspathic granodioritic orthogneisses (Gardiner *et al.* 2019; Holdsworth *et al.* 2019). Towards the north of the FSB, on the West Shetland and North Shetland platforms, the nature of the basement rock changes from crystalline to Neoproterozoic Moine and Dalradian rocks and Paleozoic Caledonian rocks (Kinny *et al.* 2005; Ritchie *et al.* 2011; Holdsworth *et al.* 2019).

Since Neoarchean pluton emplacement, crystalline basement has been subject to the complex structural evolution of the FSB. Prominent NE–SW-striking structural trends present throughout the FSB are thought to have been inherited from pre-existing structural fabrics within basement rocks. Structural fabrics are thought to have initially developed as Precambrian shear zones during the Archean and Proterozoic, which were later reactivated as both thrusts and deep-rooted strike-slip faults during the Cambrian–Devonian Caledonian Orogeny (Coward 1990; Doré *et al.* 1997). During Devonian orogenic collapse, strike-slip faults were then reactivated as normal faults (Moy and Imber 2009; Ritchie *et al.* 2011).

The predominant NE–SW-striking structural fabric has since been periodically exploited during multiple phases of crustal extension from the Permo-Triassic to the early Cenozoic (UK Atlantic margin events: Fig. 2), separating the once contiguous crystalline basement into a series of intra-basinal highs (Figs 1a and 3) (Doré *et al.* 1997, 1999; Ritchie *et al.* 2011; Ellis and Stoker 2014; Schofield *et al.* 2020).

The initial phases of sedimentary input within the FSB are attributed to the erosion of Caledonian topography into post-orogenic Devonian–Carboniferous intermontane basins, thought to have been generated by the extensional collapse of the Caledonian fold-and-thrust belt (Underhill 2003; Ritchie *et al.* 2011; Smith and Ziska 2011; Ellis and Stoker 2014; Stoker 2016). Devonian–Carboniferous-age basins (e.g. the Clair Basin on the Rona Ridge: Nichols 2005) accommodated the deposition of the Clair Group, dominated by fluvial sequences with lacustrine and aeolian influences (Underhill 2003; Smith and Ziska 2011). These deposits rest unconformably on Precambrian basement rock and form the main reservoir sequences of the Clair Field (Ogilvie *et al.* 2015; Robertson *et al.* 2020). Where penetrated by wells within the FSB on the Rona Ridge, the proven thickness of the Clair Group varies from absent (e.g. wells 205/21-1A and 206/12-1: Fig. 1b) to *c.* 1000 m thick (Ziska and Anderson 2005), reflecting a varied history of deposition and post-depositional erosion. Subsequent basin development of the FSB, after the Devonian–Carboniferous, primarily relates to the Atlantic rift system active throughout the Triassic–Cretaceous, contributing to the fragmentation of Pangaea and the opening of the Atlantic (Roberts *et al.* 1999; Ellis and Stoker 2014; Stoker 2016; Stoker *et al.* 2017*b*).

Initial rifting is indicated by large thicknesses of Permian–Triassic strata deposited within the West Orkney and Papa basins (e.g. 2436 m in well 205/27a-1: Fig. 1b) (Ritchie *et al.* 2011) and inferred from seismic profiles (Quinn and Ziska 2011; Stoker *et al.* 2017*b*). Permo-Triassic extension is thought to be concentrated within the Papa, West Shetland, West Orkney and Unst basins (Fig. 1) where Permian strata are proven (e.g. well 205/27a-1). This early rifting event is thought to have exploited existing basement structural fabrics, leading to the formation of NE–SW-trending half-graben basins filled with aeolian, fluviatile and lacustrine sequences, although differentiation of Permian–Triassic sequences is often challenging due to the lack of diagnostic biostratigraphy (Swiecicki *et al.* 1995; Štolfová and Shannon 2009; Ritchie *et al.* 2011; Stoker *et al.* 2017*b*). The presence of Permian–Triassic strata within the FSB is mostly interpreted to be concentrated around the present-day margins of the basin (e.g. wells 204/19-1, 204-19-9 and 204/29-1: Fig. 1b), with the exception of 213/23-1 (Eriboll) and 214/09-1 (Bunnehaven) which are located within the central FSB along the Corona Ridge (Quinn and Ziska 2011). Semi-arid fluvial–lacustrine conditions prevailing throughout the Triassic are expressed within the FSB as variable thicknesses of the Papa Group, ranging from 426 m within the Judd Sub-basin (204/29-1: Fig. 1b) to 73 m interpreted on the Corona Ridge by Quinn and Ziska (2011) (73 m 'indeterminate' section in well 214/09-1, Bunnehaven: ExxonMobil 2001).

Post-rift thermal subsidence coupled with global sea-level rise initiated a marine incursion during the early Jurassic, leading to the deposition of the shallow-marine Skerry Group sequences, although well penetrations of Lower Jurassic strata are sparse within the FSB (Dean *et al.* 1999; Ritchie and Varming 2011). Thermal subsidence continued until the middle–late Jurassic, when renewed extension of existing Permo-Triassic half-graben occurred, thought to be related to synchronous rifting in the North Sea (Ritchie *et al.* 2011). Numerous wells, largely confined to intra-basinal highs including

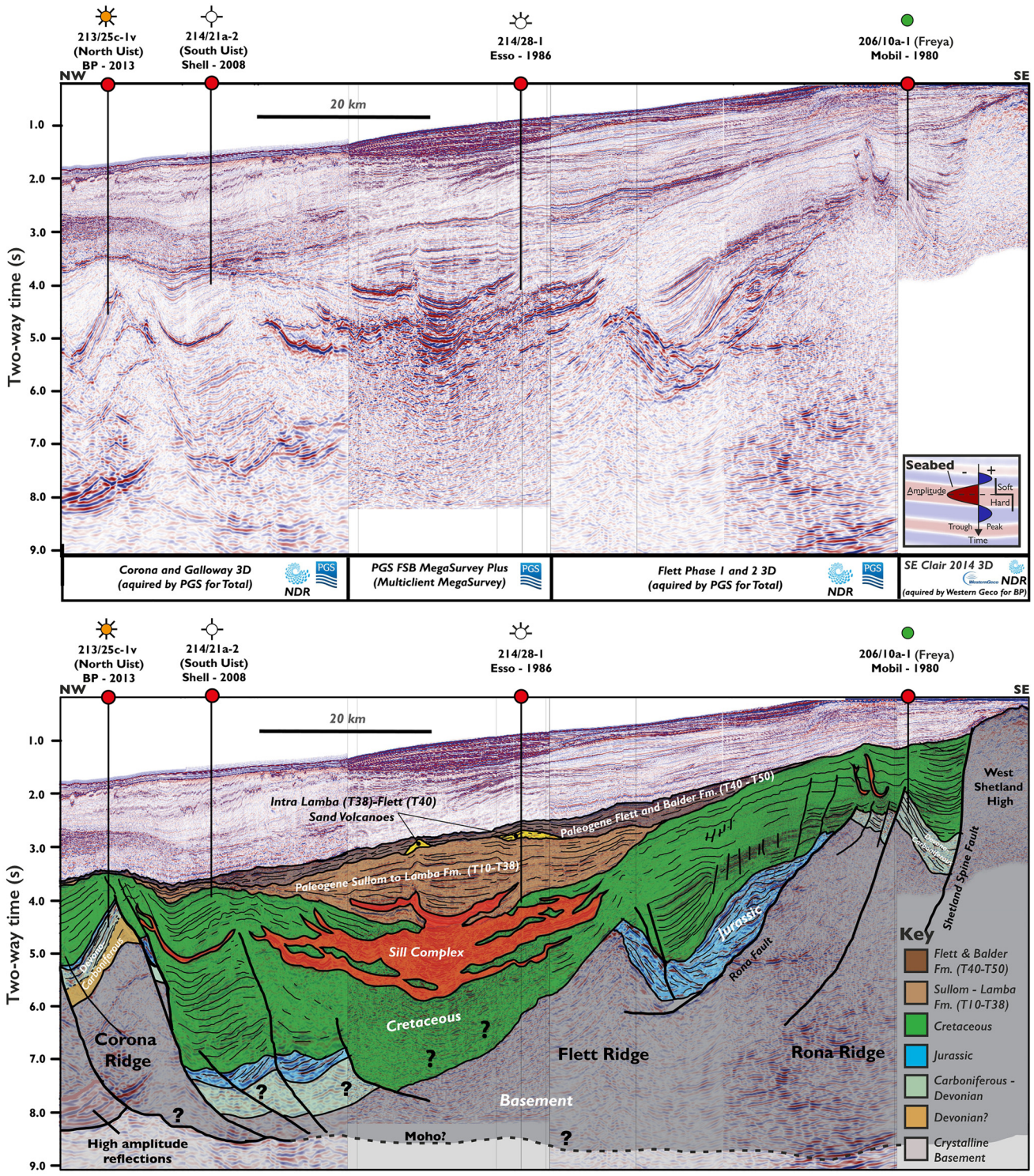

Fig. 3. NW–SE regional seismic line and geoseismic interpretation from North Uist (213/25c-1V) on the Corona Ridge, through South Uist (214/21a-2) and onto the West Shetland High. Seismic data from the North Sea Transition Authority National Data Repository were acquired by PGS for Total E&P UK Ltd and partners (Corona & Galloway 3D, Flett Phase 1 & 2 3D) and by WesternGeco (SE Clair 2014 3D) for BP and partners. The PGS FSB MegaSurvey Plus is shown courtesy of PGS who granted permission to publish the line. The location of the seismic line transect is shown in Figure 1a.

the Corona Ridge, have penetrated the Kimmeridge Formation which comprises the sand-rich Rona Sandstone Member and the organic-rich Kimmeridge Clay Member of the Humber Group (mean total organic content (TOC) of *c*. 4.5% for FSB wells: Scotchman *et al.* 1998), deposited throughout predominantly marine conditions (Ritchie and Varming 2011). The majority of the discoveries made along the Corona Ridge are thought to be sourced from the organic-rich Kimmeridge Clay (Scotchman *et al.* 2016; Gardiner *et al.* 2019).

The present-day geometry of the FSB, along with the adjacent Rockall and Møre basins, was mainly developed by widespread extension initiated within the early Cretaceous, which is largely responsible for the present-day structure of the Corona Ridge (Ritchie *et al.* 2011; Hardman *et al.* 2018). Extension along the NE Atlantic margin during the Cretaceous was concurrent with northward propagation of the Central Atlantic rift system, which became relatively inactive after the late Cretaceous period (Doré *et al.* 1999; Fletcher *et al.* 2013; Stoker 2016; Schofield *et al.* 2020).

Deposition of thick (up to 5 km) deep-marine Cretaceous successions occurred on the hanging walls of major fault systems (Larsen *et al.* 2010; Stoker 2016; Gardiner *et al.* 2019).

Post-rift thermal subsidence was terminated by a rifting phase during the early Paleocene (concentrated 400 km to the west) which exploited the established Mesozoic normal rift system and occasionally manifests on the Corona Ridge as minor normal faulting on reactivated major bounding faults only (Doré *et al.* 1999; Smallwood and Gill 2002; Ellis and Stoker 2014). The NE Atlantic margin experienced significant igneous activity during the Paleocene–Eocene, prior to (*c.* 62–58.5 Ma) and during (*c.* 57–54 Ma) continental break-up between Greenland and NW Europe (Watson *et al.* 2017; Jolley *et al.* 2021).

This study employs the British Geological Survey (BGS) lithostratigraphy from Ritchie *et al.* (2011), which adopts the BP Paleocene T-sequence framework of Ebdon *et al.* (1995) (Fig. 4) for consistency with previous studies. The regional onset of volcanism within the FSB occurred prior to continental break-up and is recorded by Danian (66–61.6 Ma) to Selandian (61.6–59.2 Ma) basaltic tuffs of sequences T10–T36 (Watson *et al.* 2017; Jolley *et al.* 2021). Marine conditions prevailed throughout the Paleocene, accompanied by the deposition of a series of major turbidite fans in adjacent basins (e.g. the Flett, Judd and Nuevo sub-basins) during the mid-Paleocene (sequence T31–T36) (Stoker and Varming 2011).

Rifting was followed by uplift that began during the late Paleocene (Ebdon *et al.* 1995). Subsequent emergence of areas adjacent to the FSB (e.g. the East and West Shetland platforms) facilitated the deposition of Thanetian (59.2–56 Ma) to Ypresian (56–47.8 Ma) major prograding shelf-margin systems (sequences T38–T40) during the late Paleocene–early Eocene (Stoker and Varming 2011).

The main phase of extrusive volcanism occurred within the early Eocene during continental break-up, with the eruption of a widespread extrusive basaltic component comprised predominantly of thick flood basalt (lava) sequences of the Faroe Islands Basalt Group (FIBG) (Bell and Jolley 1997; Passey and Hitchen 2011; Schofield *et al.* 2017; Jolley *et al.* 2021). Flood basalt eruption during the deposition of Colsay Member sandstone units (sequence T40–T45) led to the formation of intra-basaltic plays of the Rosebank Field located along the Corona Ridge (Jolley and Bell 2002; Passey and Jolley 2009; Schofield and Jolley 2013; Hardman *et al.* 2018). The emplacement of an extensive suite of mafic intrusions, the Faroe Shetland Sill Complex (FSSC), occurred before and during continental break-up between *c.* 58 and 55 Ma (Schofield *et al.* 2017; Watson *et al.* 2017; Jolley *et al.* 2021).

A migration of the Central Atlantic rift system extension locus to the west of the present-day Faroes occurred during the early Eocene, synchronous with the onset of North Atlantic seafloor spreading between *c.* 56 and 55 Ma (Ellis and Stoker 2014; Stoker *et al.* 2017*a*, *b*; Jolley *et al.* 2021). Supra-basaltic Hildasay Member (sequence T45) sandstones of the Flett Formation are overlain by the Balder Formation (sequence T50), which acts as a regional seismic marker (Ebdon *et al.* 1995; Watson *et al.* 2017). A return to deep-marine conditions in the early Eocene resulted in the deposition of the Stronsay Group (sequence T60–T98: Stoker *et al.* 2012), which contains a number of submarine fan complexes including the mid-Eocene Breydon, Caledonia, Rothbury and Strachan fans, that have proven to be sandstone rich along the Corona Ridge, with the latter a reservoir for the Tobermory gas field (Mobil North Sea Ltd 1999*a*, *b*; Smallwood and Gill 2002; Stoker and Varming 2011).

The FSB was subject to multiple further episodes of tectonism during the late Paleocene, early–mid-Eocene and Oligo-Miocene (Smallwood and Maresh 2002; Smallwood 2004; Ellis *et al.* 2009). Throughout this time, inversion along intra-basinal highs facilitated the growth of elongate anticlines and domal structures with four-way closures within Cretaceous–Cenozoic-age strata (Sørensen

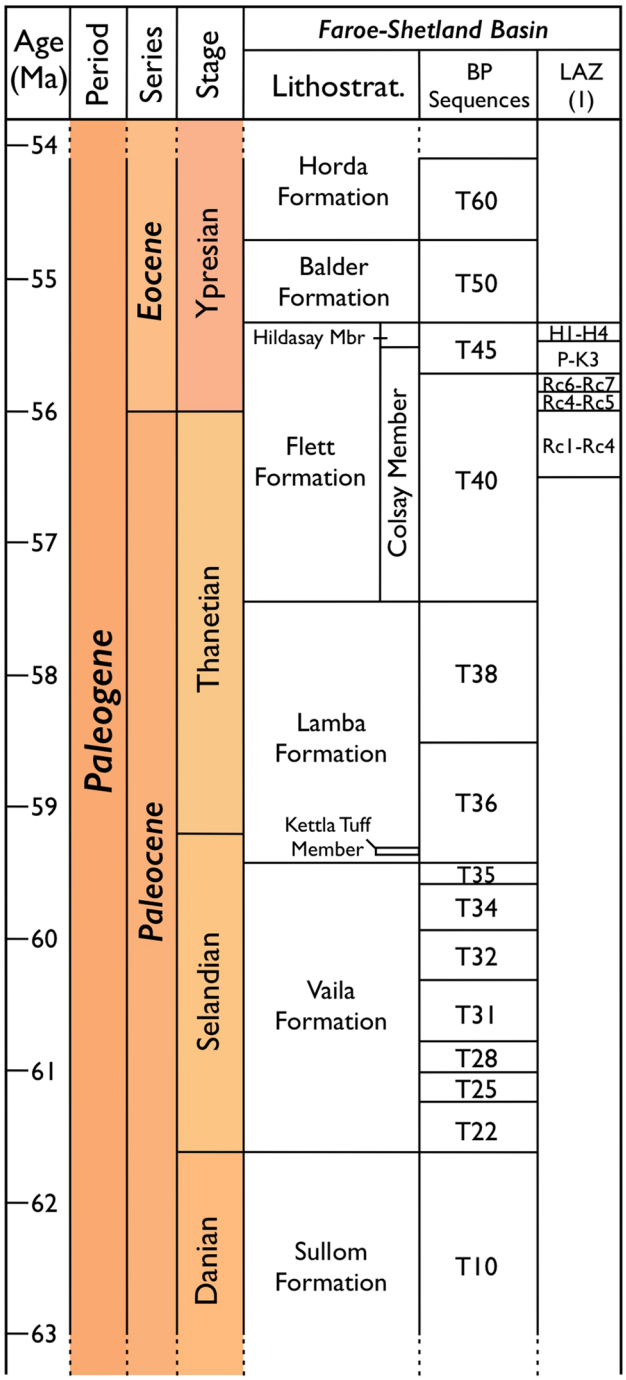

Fig. 4. Paleogene stratigraphy of the Faroe–Shetland Basin, with the British Geological Survey (Ritchie *et al.* 2011) and BP T-sequence framework (after Ebdon *et al.* 1995) modified from Schofield and Jolley (2013) and Jolley *et al.* (2021). The local assemblage zone, LAZ (1), was defined by Schofield and Jolley (2013) and updated by Jolley *et al.* (2021).

2003; Doré *et al.* 2008; Ritchie *et al.* 2008). This inversion is most likely to have been responsible for many of the traps present along the Corona Ridge but is also considered to be responsible for the breach of pre-existing top seals and subsequent leakage (Ritchie *et al.* 2011; Ellis and Stoker 2014; Stoker *et al.* 2017*a*).

Previous structural interpretation of the Corona Ridge

The most prominent structural elements in the FSB are the NE–SW-trending intra-basinal highs composed of Precambrian crystalline basement including the Corona Ridge (and other structural highs such as the Rona Ridge). In this study we follow the definition of

basement high proposed by Peacock and Banks (2020, p. 18), 'an area in which the basement rocks [Precambrian crystalline rocks] are significantly higher than in the surrounding areas'. Within the Peacock and Banks (2020) definition, the word 'significantly' is used in the context of influencing the petroleum system (e.g. source rock maturation and subsequent migration). The term 'central-northern Corona Ridge' is used herein to refer solely to the Precambrian crystalline rocks that form the intra-basinal high itself.

Rumph *et al.* (1993) introduced the term Corona Ridge, although the ridge was previously variably referred to as the Mid-Faeroe Ridge (Mudge and Rashid 1987; British Geological Survey 1996; Hughes *et al.* 1997), Central High Complex (Hitchen and Ritchie 1987), Axial Opaque Zone (Ridd 1981, 1983) and North Westray Ridge (Iliffe *et al.* 1999). Early conceptual models for the development of the Corona Ridge include a Cenozoic igneous complex similar to the Wyville–Thomson Ridge (Ridd 1981; Hitchen and Ritchie 1987) or, as the Corona Ridge is now known, a Lewisian-age crystalline basement-cored structural high analogous to the Rona Ridge (Mudge and Rashid 1987).

Numerous authors extend the ridge SW to the Cambo High (Ellis *et al.* 2009; Ritchie *et al.* 2011; Hardman *et al.* 2018) and NE towards Quadrant 217 (Mudge and Rashid 1987; BGS 1996; Hughes *et al.* 1997; Dean *et al.* 1999; Ellis *et al.* 2009; Ritchie *et al.* 2011). The complexity of the Corona Ridge varies between publications. Many publications (Mudge and Rashid 1987; Rumph *et al.* 1993; Ebdon *et al.* 1995; BGS 1996; Hughes *et al.* 1997; Dean *et al.* 1999; Ritchie *et al.* 2011) describe the Corona Ridge as comprising one or two linear NE–SW-trending basinal highs, totalling *c.* 100–150 km in length, bound by NE–SW-striking faults and delineated only by the Victory Lineament transfer zone (Rumph *et al.* 1993; Ebdon *et al.* 1995; Ritchie *et al.* 2011). Within other publications the Corona Ridge is presented as a more complex structure with three structurally separate blocks (Fig. 1) (Ellis *et al.* 2009). Ellis *et al.* (2009) interpreted the Corona Ridge as one NE–SW-trending feature (Fig. 1) bound by NE–SW-striking faults, which bifurcates within Quadrant 214 into two separate highs, each extending towards Quadrant 217, which bound the Sissal Sub-basin (denoted as SB in Fig. 1). Within the study area, however, according to Ellis *et al.* (2009), the Corona Ridge comprises one NE–SW-trending high (Fig. 1).

Recent publications investigating the crystalline basement structure within the FSB (e.g. Rippington *et al.* 2015; Schofield *et al.* 2017; Holdsworth *et al.* 2019; Peacock and Banks 2020) often focus on other prospective structural highs in the basin (e.g. the Rona Ridge). Publications that are focused on the Corona Ridge itself (e.g. Hardwick *et al.* 2010) describe reprocessing methods to improve seismic imaging of the complex Corona Ridge. However, at the time of publication, no detailed maps showing the structural complexity of the Corona Ridge have been published.

Although the characterization along the southern Corona Ridge has improved through time due to the drilling of the three deep penetrating Rosebank exploration and appraisal wells (213/27-1Z, 213/27-2 and 213/27-3Z), knowledge of the structural configuration, geology and hydrocarbon prospectivity of the central-northern Corona Ridge is still enigmatic. The work presented here shows that the along-strike structural configuration of the Corona Ridge is much more complex than previously thought, as will be discussed below.

Data and methodology

The main seismic data used for interpretation throughout this project, and shown here in Figures 5–8, is a broadband 3D seismic survey acquired by PGS (Petroleum Geo-Services) for Total E&P UK Ltd and partners in two phases; phase 1 in 2013 (Galloway) and phase 2 in 2015 (Corona) (Joseph *et al.* 2017). The key parameters of each acquisition phase are summarized in Table 1, and the area covered by the survey is shown in Figure 1.

Data are displayed at zero-phase negative standard (Sheriff and Geldart 1982) European polarity, with a downward increase in acoustic impedance (hard) corresponding to a negative amplitude (trough) displayed in red and a downward decrease in acoustic impedance (soft) corresponding to a positive amplitude (peak) displayed in blue. Near the Top Paleocene, at 3.5 s two-way time (TWT) (*c.* 3.5 km depth), the dominant frequency is 22 Hz, giving a vertical resolution of *c.* 37.5 m (assuming a velocity of 3300 m s^{-1} for the Paleocene: Rippington *et al.* 2015). Towards the base Cretaceous at 6.5 s TWT (*c.* 12 km depth) within the Flett Sub-basin the dominant frequency drops to 8 Hz, giving a vertical resolution of *c.* 147 m (assuming a velocity of 4700 m s^{-1} for the Cretaceous: Rippington *et al.* 2015). Towards the base of the survey at 8 s TWT (*c.* 18 km depth) the dominant frequency drops further to *c.* 6 Hz, giving a vertical resolution of *c.* 270 m (assuming a velocity of 6500 m s^{-1} for the crystalline crust: Rippington *et al.* 2015). Seismic data extend down to 10 s TWT.

Three exploration wells drilled along the central-northern Corona Ridge were used throughout this study: 213/23-1 (Eriboll), 214/21a-2 (South Uist) and 213/23c-1V (North Uist). Well data were downloaded from the NSTA National Data Repository (North Sea Transition Authority 2022), where it is freely available. The wells within this paper were drilled as near-vertical exploration wells, and throughout this paper the depths are quoted in measured depth (MD (m)), unless otherwise specified. We have completed a detailed reinterpretation of well data including end of well reports, wireline data, composite logs, image logs, core and biostratigraphy (where available) to allow the wells to be placed in the stratigraphic context of the NE Atlantic margin (see Jolley *et al.* 2021), and, in particular, in the context of the detailed stratigraphy of the Rosebank Field (after Schofield and Jolley 2013).

Central-Northern Corona Ridge exploration wells

213/23-1 (Eriboll)

213/23-1 (Eriboll) was the first well drilled along the Corona Ridge, in July 1998 by Mobil. The well targeted three stratigraphic intervals: the primary Mesozoic-age Eriboll oil prospect on the footwall of a tilted fault block (the Corona Ridge) with three-way dip closure, and two shallower secondary targets within the upper Paleocene (Solway prospect) and middle Eocene (Caledonia prospect) (Mobil North Sea Ltd 1999*a*). Pre-drill concerns regarding timing, migration and lack of charge of the secondary targets were confirmed by the presence of water within the upper Paleocene Solway and middle Eocene Caledonia prospects. The well encountered Eocene–Paleocene strata, Cretaceous strata, a section postulated to be Triassic strata (referred to as 'Triassic?' in the end of well report) and Devonian–Carboniferous strata. No Jurassic strata were penetrated in the well (Mobil North Sea Ltd 1999*a*). According to the end of well report, 213/23-1 (Eriboll) penetrated 1.5 m of rock assigned as Precambrian Lewisian gneiss before reaching total depth (TD) at 4344 m MD. However, cuttings of the 1.5 m of Lewisian basement are described within the end of well report as both 'crystalline and porphyritic' and to contain 'lithic fragments' (Mobil North Sea Ltd 1999*a*). Numerous oil shows were encountered within Upper Cretaceous, 'Triassic?' and Devonian–Carboniferous strata.

213/23-1 (Eriboll) – Paleocene–Eocene: identification of the T40–T45 Colsay Member and Colsay units 1–4

Our reinterpretation of various types of well data (specifically biostratigraphy suggestive of depositional environments associated with Colsay units 1–4) obtained from 213/23-1 has allowed

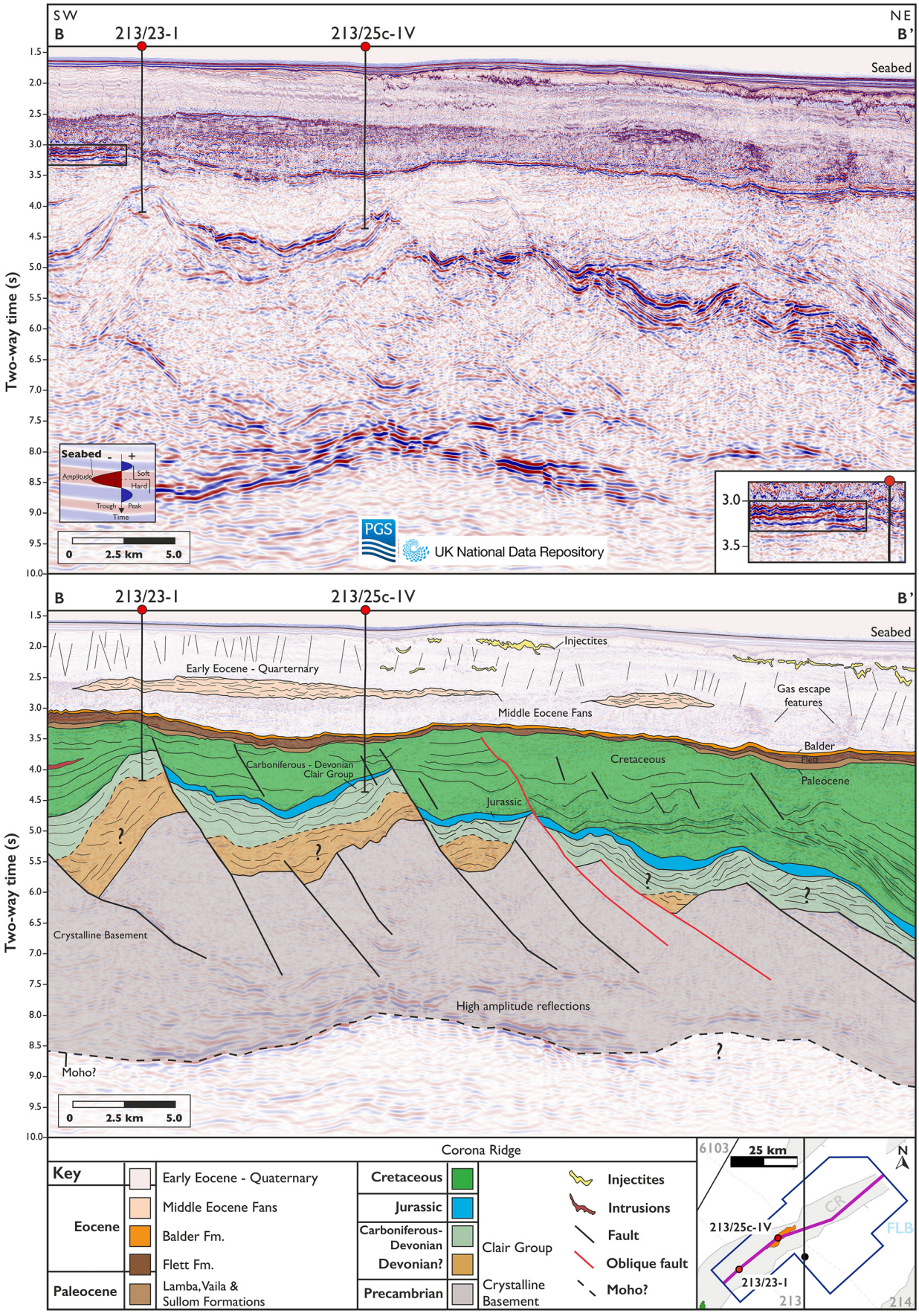

Fig. 5. NE–SW 3D Corona seismic line and geoseismic interpretation through the central-northern Corona Ridge, and exploration wells 213/23-1 (Eriboll) and 213/23c-1V (North Uist). Seismic data were acquired by PGS for Total E&P UK Ltd and partners and is from the North Sea Transition Authority National Data Repository. The location of the seismic line transect is shown in Figure 1a. Note: (1) faults shown in red correspond to oblique north–south- and NNW–SSE-trending faults at Top Crystalline Basement (Fig. 14); and (2) the black outline on the seismic section (top left at *c*. 3s TWT) highlights the presence of a similar Flett Formation seismic response to that of the Rosebank Field (Hardman *et al.* 2018, p. 77, fig. 7a; Poppitt *et al.* 2018, p. 378, fig. 6; Duncan *et al.* 2020, p. 985, fig. 6).

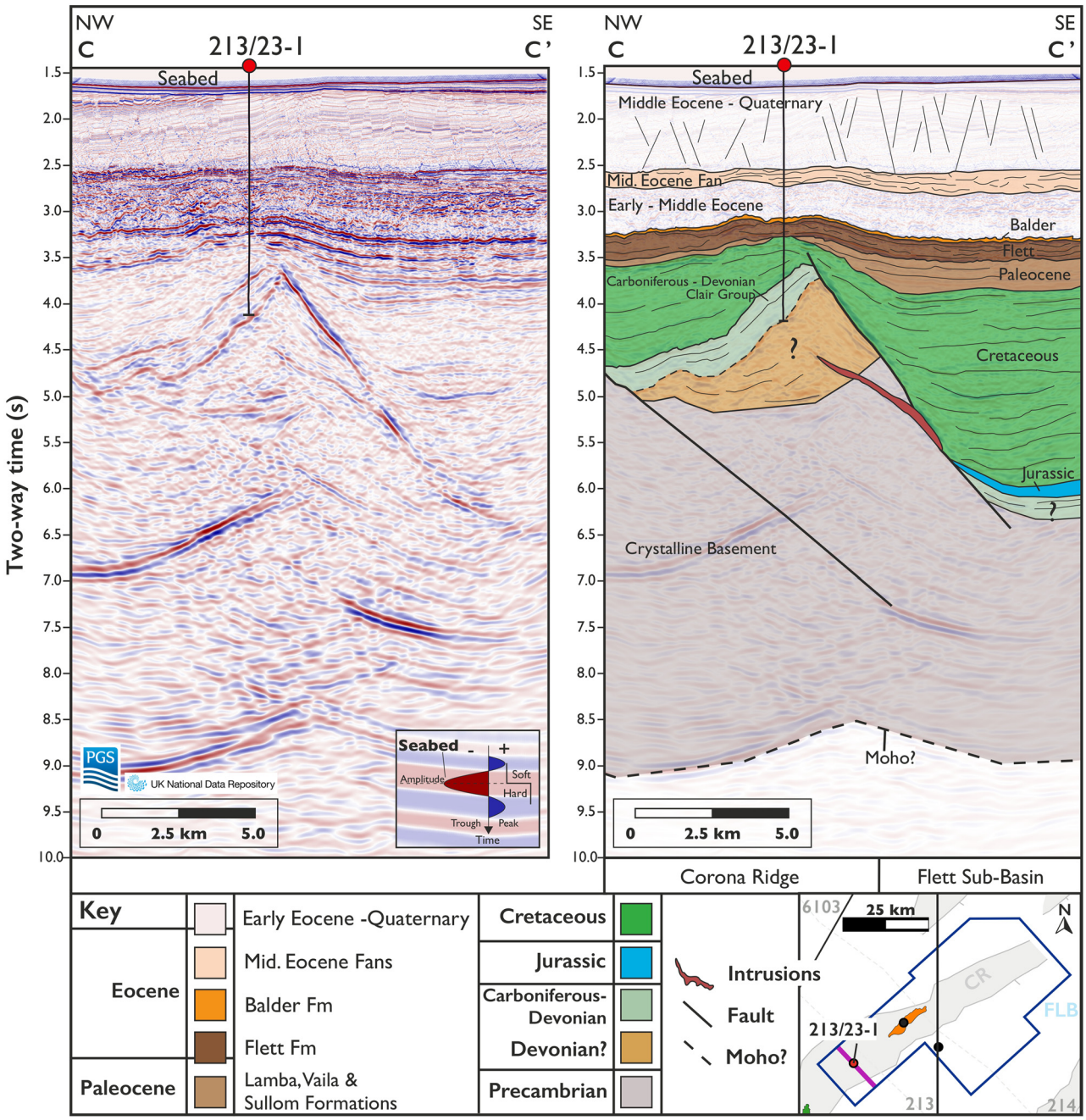

Fig. 6. NW–SE 3D Corona seismic line and geoseismic interpretation through the central-northern Corona Ridge, well 213/23-1 (Eriboll) and the Flett Sub-basin. Seismic data were acquired by PGS for Total E&P UK Ltd and partners and is from the North Sea Transition Authority National Data Repository. The location of the seismic line transect is shown in Figure 1a.

sequences penetrated within the well to be assigned to the current Paleocene–Eocene lithostratigraphic framework (Ritchie *et al.* 2011; Schofield and Jolley 2013) and T-sequences (Ebdon *et al.* 1995) used throughout the FSB (Fig. 4), not assigned at the time the well was drilled.

By re-evaluating biostratigraphy, we found that the Horda Formation (sequence T60, Ypresian age), not previously identified, lies conformably on the Balder Formation (sequence T50), which comprises claystone with thin beds of volcanic tephra. The upper Paleocene Solway prospect was prognosed between the Balder and Flett formations. The Solway prospect, which was thought to be hosted in shallow-marine sandstones, was also found to be dry (Mobil North Sea Ltd 1999*a*).

We found that the well (213/23-1, Eriboll) encountered 422 m of Flett Formation; more than double the original thickness interpreted post-drill (194 m) (Fig. 9a). No oil shows were observed within the 42 m-thick upper section of the Flett Formation, which we assigned to the Hildasay Member (sequence T45). The well (213/23-1) penetrated a 380 m-thick section that we assigned to the Colsay Member (sequence T40–T45) of the Flett Formation, which is comparable in thickness to the Colsay interval throughout the Rosebank Field (*c.* 400 m: ChevronTexaco Upstream Europe 2004; Chevron Upstream Europe 2007*a*). Within 213/23-1 (Eriboll), the Colsay interval is described in the end of well report as a series of sandstones interbedded with mudstones and siltstones (Mobil North Sea Ltd 1999*a*). Numerous traces of residual oil within the lower (sequence T40) Colsay Member were observed (Fig. 10).

According to the end of well report, the well (213/23-1) encountered the Lamba Formation (sequence T36–T38) and an undifferentiated Paleocene-aged tuffaceous unit below the Flett Formation (Fig. 9a) (Mobil North Sea Ltd 1999*a*). However, our biostratigraphic reinterpretation suggests that both intervals actually

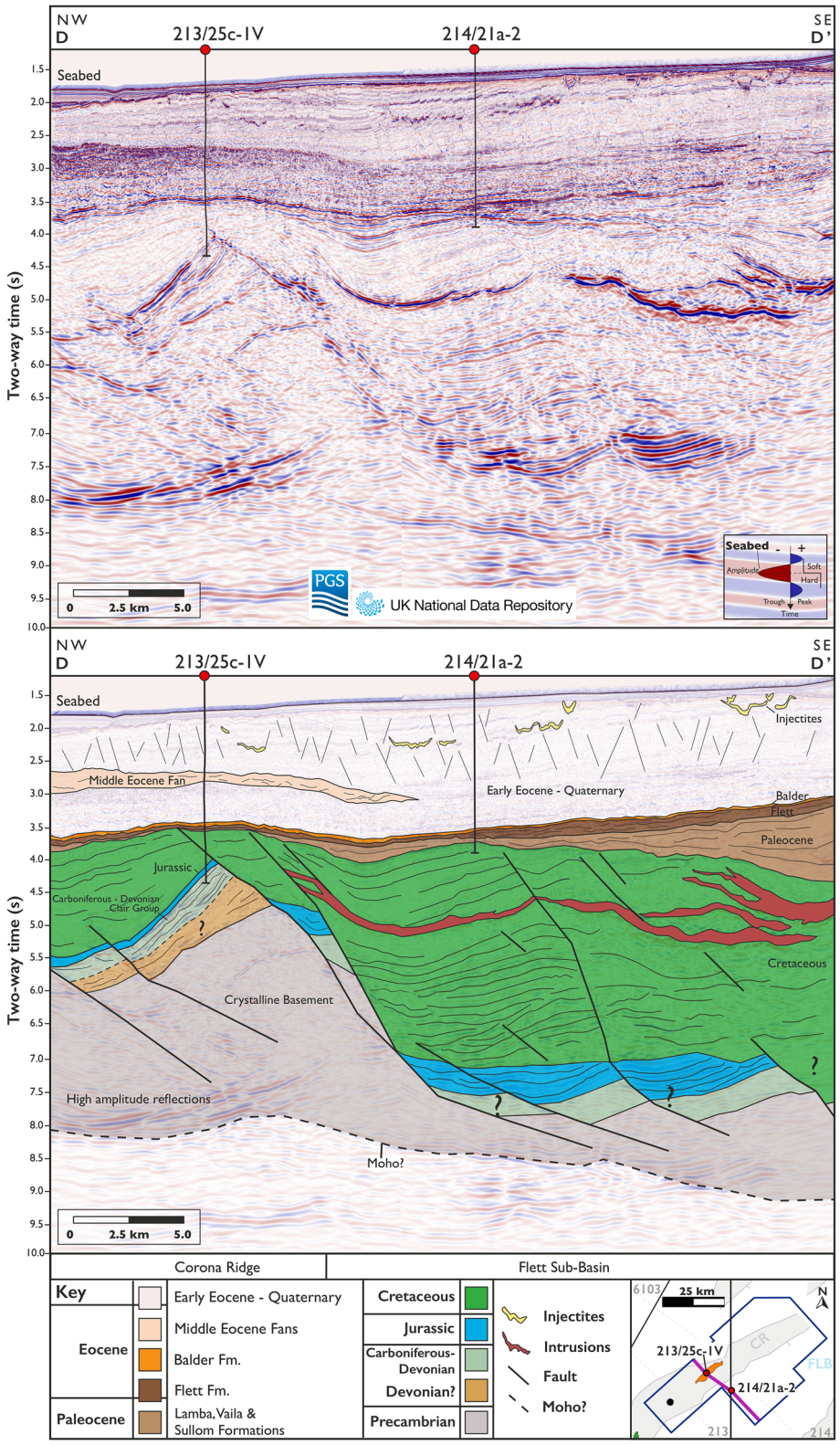

Fig. 7. NW–SE 3D Corona seismic line and geoseismic interpretation through well 213/25c-1V (North Uist) on the central-northern Corona Ridge and well 214/21a-2 (South Uist) drilled just off the central-northern Corona Ridge within the Flett Sub-basin. Seismic data were acquired by PGS for Total E&P UK Ltd and partners and is from the North Sea Transition Authority National Data Repository. The location of the seismic line transect is shown in Figure 1a.

represent the T40 Colsay 4 unit interval (Fig. 10) and that no T10–T38 sequences are present within the well. The Colsay 4 unit comprises material eroded and reworked from Paleocene-aged (sequence T10–T38) sediments.

Reinterpretation of the Colsay Member (sequence T40–T45) within 213/23-1 (Eriboll) using the end of well report, composite log, biostratigraphy and resistivity image logs has facilitated the identification of a series of sequence T40 volcanic rocks, and sub-basaltic and intra-basaltic sandstones. Biostratigraphic interpretation of two Rosebank wells (appraisal well 213/27-2 and exploration well 213/27-3Z) was used to correlate the Colsay intervals 21.3 km along the central-northern Corona Ridge from the Rosebank Field to 213/23-1 (Eriboll) (Fig. 11). Descriptions of each Colsay unit (units 1–4) within 213/23-1 are given within Table 2.

213/23-1 (Eriboll) – Paleocene–Eocene: identification of T40–T45 Colsay Member volcanic intervals

According to the original composite log, two 2–3 m-thick sections of 'intrusive volcanics' identified as 'dolerite? volcanics?' were

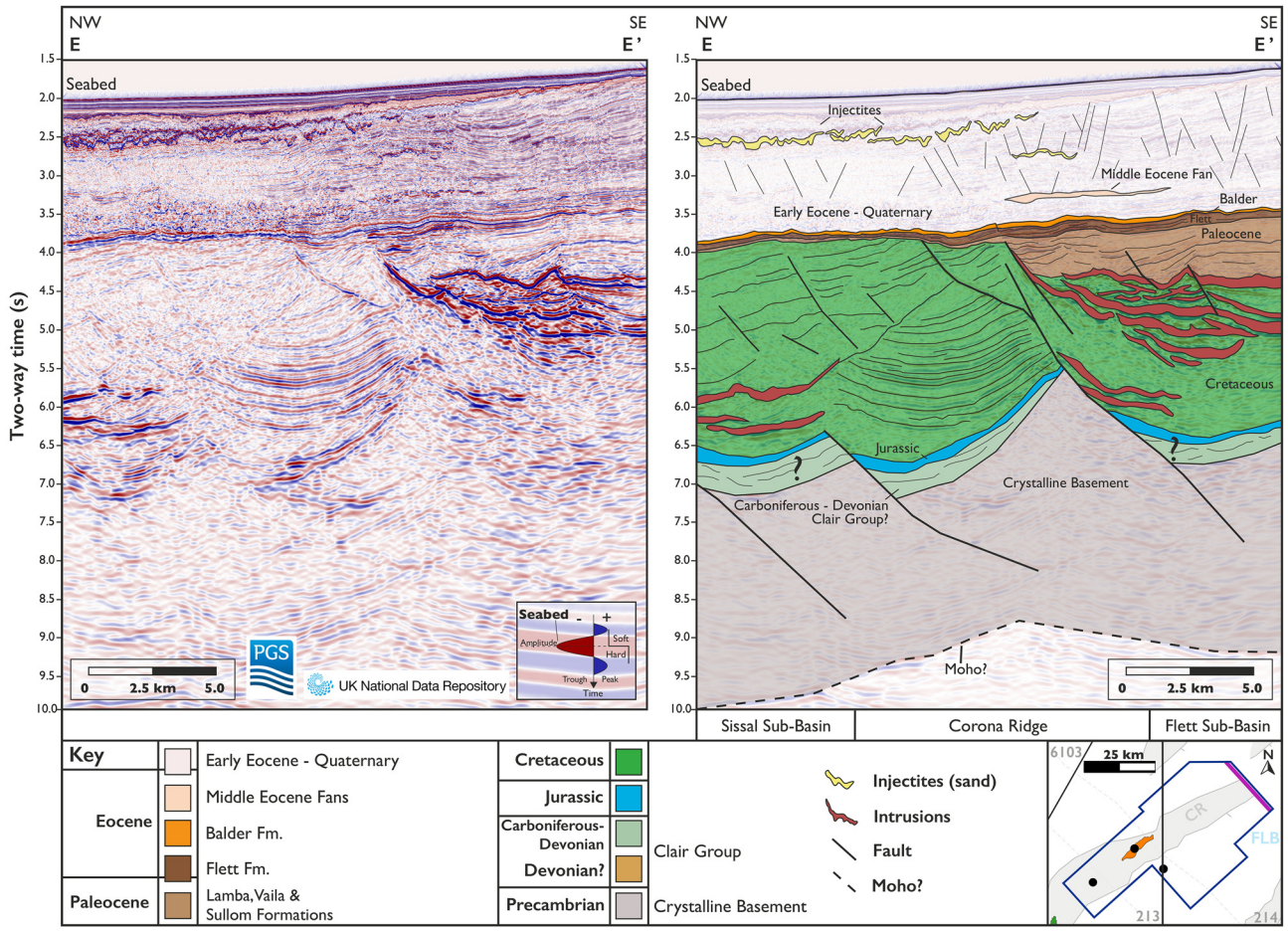

Fig. 8. NW–SE seismic line and geoseismic interpretation through the central-northern Corona Ridge within the NW end of the dataset. Note the unusual Cretaceous seismic response (usually opaque mudstones), possibly reflecting sand–claystone intervals or limestone 'stringers'. Seismic data were acquired by PGS for Total E&P UK Ltd and partners and is from the North Sea Transition Authority National Data Repository. The location of the seismic line transect is shown in Figure 1a.

penetrated between 2870 and 2890 m MD (2840–2860 m TVDSS (true vertical depth subsea)) (Figs 9 and 10), within an 18 m-thick limestone host rock. Cuttings of the 'intrusive volcanics' are described within the composite log as 'black-grey, translucent, opaque, brown, locally green, black mafic groundmass, hard, crystalline to very finely crystalline, equigranular, trace mica and pyrite, no porosity'. However, a core plug taken within the upper 'intrusive volcanic' section is contrastingly identified as claystone in the end of well report (Mobil North Sea Ltd 1998, 1999*a*). Core plugs taken within the proposed limestone section are also contrastingly identified as siltstone and dolerite within the end of well report (Fig. 10). As a result of these discrepancies, we reinterpreted lithologies throughout the entire Colsay Member (T40–T45) interval using wireline, composite log, core plug, core and resistivity image log data (Fig. 10). We interpreted four volcanic intervals (Fig. 10) that were previously interpreted as either sandstone or limestone intervals in the original composite logs (Mobil North Sea Ltd 1998).

The reinterpreted volcanic intervals are typified by low gamma-ray values and fast sonic values (Fig. 10). Resistivity image logs of the volcanic intervals contain *c.* 10 cm-wide conductive zones that are likely to represent open fractures or cooling joints (Fig. 10c, e), whilst other volcanic intervals (Fig. 10a, c) have thinner (<1 cm wide) vertical conductive (open) fractures (possibly drilling induced). The thickness of laminated claystone overlying the volcanic intervals appears to have been influenced by the underlying rough top surface of lava observed within the image logs (Fig. 10f), suggesting that the intervals within well 213/23-1 (Eriboll) are lava flows, not igneous intrusions, as suggested for the two 2–3 m-thick sections described as 'intrusive volcanics' within the original composite log (Fig. 10) (Mobil North Sea Ltd 1998).

213/23-1 (Eriboll) – Cretaceous

Petrophysical analysis completed by Mobil suggests that Upper Cretaceous Cenomanian–Turonian Shetland Group sandstones are oil bearing and contain 4.9 m of net pay (Mobil North Sea Ltd 1999*a*). No oil shows were recorded within the 19.5 m-thick Lower Cretaceous Cromer Knoll Group. The Lower Cretaceous claystone lies unconformably on strata identified as 'Triassic?' within the end of well report (Mobil North Sea Ltd 1999*a*).

Table 1. *Key acquisition parameters of phase 1 and 2 of the 3D seismic survey used in this study (PGS Geophysical 2013, 2015)*

Acquisition parameters	Phase 1: Galloway 2013	Phase 2: Corona 2015
Dual source depth (m)	9	9
Number of streamers	12	10
Streamer towing depth (m)	20	20
Streamer spacing (m)	100	100
Streamer cable length (m)	6000	7050
Near trace offset (m)	200	99
Shot interval (m)	25	25

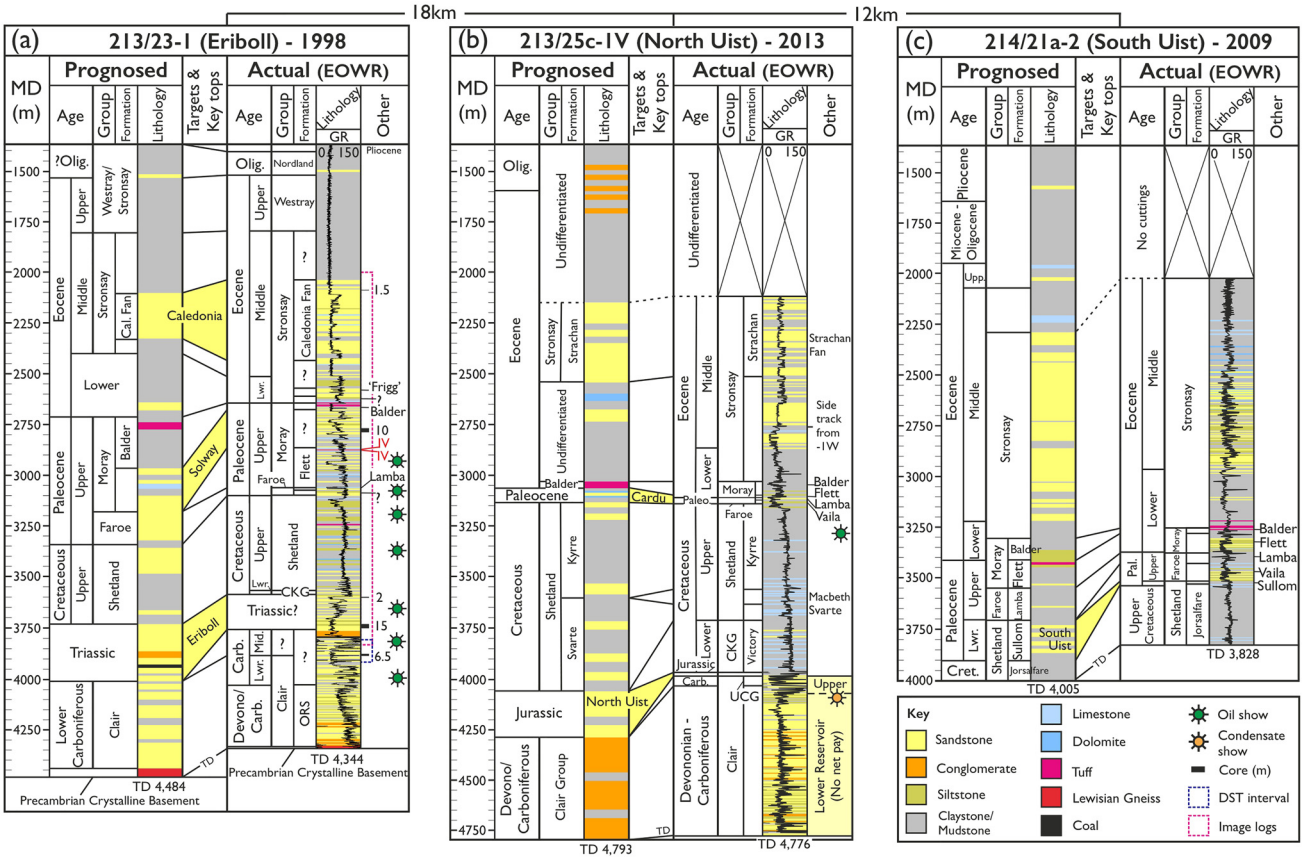

Fig. 9. Pre-drill (prognosed) and post-drill (actual) lithologies (with gamma ray) and lithostratigraphy of wells (**a**) 213/23-1 (Eriboll), (**b**) 213/23c-1V (North Uist) and (**c**) 214/21a-2 (South Uist) with relevant well data obtained, and hydrocarbon shows encountered. Note the inconsistencies in well tops: for example, the Top Paleocene varying between the Top Balder Formation (213/23-1), the Top Flett Formation (213/25c-1V) and the Top Lamba Formation (214/21a-2). Prognosed (pre-drill) and actual (post-drill) lithostratigraphy and well tops are unmodified from those given within composite logs and end of well reports (Mobil North Sea 1999*a*; Shell UK Ltd 2010; BP Exploration Operating Company Ltd 2013*b*). Abbreviations; CKG, Cromer Knoll Group; EOWR, end of well report; IV, 'Intrusive Volcanics?'; ORS, Old Red Sandstone; TD, total depth; UCG, Upper Clair Group; ?, undifferentiated.

213/23-1 (Eriboll) – does 213/23-1 penetrate a Triassic sequence?

The Triassic interval (*c.* 3585–3763 m MD) is assigned with uncertainty according to the end of well report and is referred to as 'Triassic?', although there is no biostratigraphic evidence for the assignation of a Triassic age to this section. The original biostratigraphic analysis states that 'palynological evidence suggests Carboniferous aged sediments may be present, but the results are not conclusive' in regard to the section assigned 'Triassic?' (Mobil North Sea Ltd 1999*b*, p. 3). Within the 'Triassic?' section (at 3736 m MD: Fig. 12), '*in situ* Carboniferous taxa' are recorded, although considered sparse, and the interval remained lithostratigraphically unassigned as such (Mobil North Sea Ltd 1999*b*, p. 45). Two separate interpretations of the interval are provided in the post-well biostratigraphic analysis: either a continuation of the Lower Cretaceous Cromer Knoll Group or the section being middle Carboniferous in age (Mobil North Sea Ltd 1999*b*, p. 2). A continuation of Lower Cretaceous strata is unlikely due to the seismic observation that the Cromer Knoll Group lies at an apparent angular unconformably to the proposed 'Triassic?' section (Fig. 6). The absence of any unconformity within resistivity logs at and proximal to the proposed 'Triassic?'–middle Carboniferous boundary (pink dashed line, 3763 m MD: Fig. 12a) and the similarity of facies and bedding (orientation and dip) within both the 'Triassic?' and middle Carboniferous section suggests that the 'Triassic?' section may instead be a continuation of underlying middle Carboniferous strata (Mobil North Sea Ltd 1999*a*). We therefore interpret the 'Triassic?' interval within 213/23-1 (Eriboll) as a continuation of the underlying middle Carboniferous Clair Group strata identified within the original end of well report (Fig. 13) and this is discussed in the following subsection.

213/23-1 (Eriboll) – Carboniferous

The middle Carboniferous (Clair Group) is described within the end of well report as a series of homogenous sandstones with good (*c.* 15%) porosities, conglomerates, laminated mudstones and one 5 m-thick interval of coal (Mobil North Sea Ltd 1999*a*). Fining-up sequences containing flat to low-angle bedding and cross-bedding with localized mud clasts and burrows are evident within core obtained from the interval (Mobil North Sea Ltd 1999*c*). We interpret the presence of coal, laminated mudstones, conglomerate, and cross-bedded sandstones containing mud clasts and burrows as having been deposited within a fluvial depositional environment (Mobil North Sea Ltd 1999*c*). Coal is also present within the age-equivalent fluvial–fluviodeltaic Carboniferous sequences of the Clair Field (Robertson *et al.* 2020). Post-drill petrography of middle Carboniferous core (Fig. 12) suggests that lower porosities (<2.5%) are present, the result of *c.* 1 m-thick sections exhibiting extensive dolomite and calcite cement (Fig. 12), and the presence of matrix clay and quartz overgrowth cement (Mobil North Sea Ltd 1999*c*). Oil shows were encountered within the middle Carboniferous interval, with oil described as 'bubbling' from core (Fig. 12) (Mobil North Sea Ltd 1999*a*) and traces of oil were seen in mud at the shakers (3876–3884 m MD) (Mobile North Sea Ltd 1999*a*).

Lower Carboniferous strata are characterized within the composite log by sandstones with fair to good porosity, recorded as

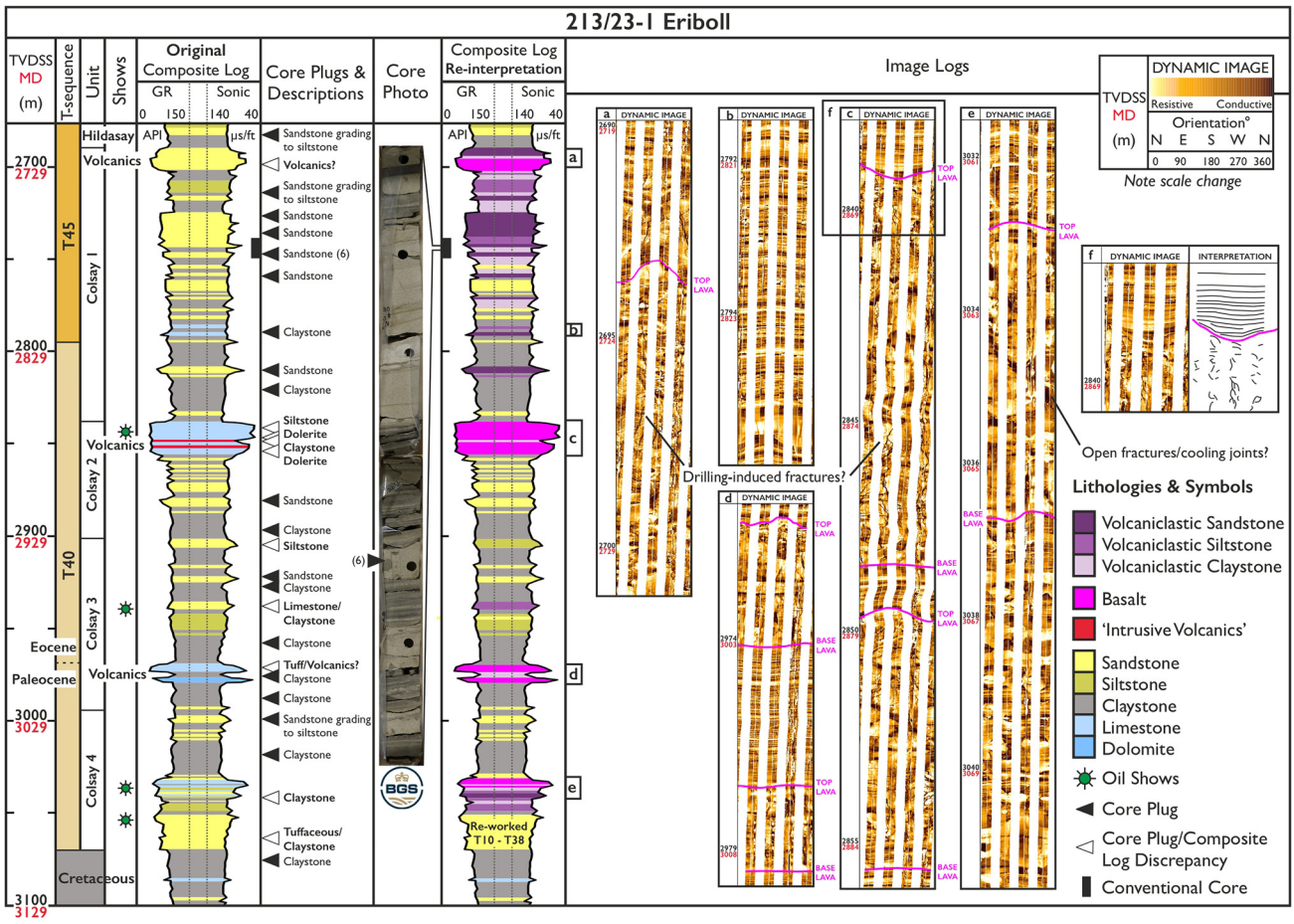

Fig. 10. Original composite log lithologies (also see Fig. 9a) and reinterpreted lithologies of the Colsay Member (sequence T40–T45) within well 213/23-1 (Eriboll) with relevant intervals of resistivity image logs used to reinterpret the section. Note: (1) Colsay units 1–4 were assigned based on biostratigraphy suggestive of different depositional environments generally associated with each unit; (2) where core-plug lithology is not consistent with composite log lithology, lithology is listed in bold; (3) the different depth scales of resistivity image logs; and (4) for the location of (f), see (c).

containing oil shows (Mobil North Sea Ltd 1998). No image logs or core were obtained through the lower Carboniferous section. Average petrophysical properties throughout the Carboniferous section are shown in Table 3.

Despite some Carboniferous fractures (Fig. 12) exhibiting residual brown and black oil stains, the reservoir quality of the unit is considered poor due to the presence of dolomite cement, calcite cement and clay smears (Mobil North Sea Ltd 1999*c*). We interpret fractures present within resistivity image logs of the middle Carboniferous strata to have dominant strike orientations of NE–SW and ENE-WSW (Fig. 12b). Fracture density is higher within the uppermost section of the middle Carboniferous (1 m^{-1}) previously interpreted as 'Triassic?' (3585–3763 m MD) compared with the lowermost middle Carboniferous section (0.5 m^{-1} at 3763–3884 m MD), although borehole washouts impaired image log interpretation within the lower section (Fig. 12). We interpret borehole breakouts with NE–SW orientations and drilling-induced tensile fractures (DITFs) with NW–SE orientations within middle Carboniferous strata as suggesting a present-day maximum horizontal stress ($S_{H\,max}$) orientation of NW–SE.

A drill stem test (DST) was later performed on the lower–middle Carboniferous prospective 'Eriboll Middle Zone' from depths of 3814 to 3914 m MD (Figs 9a and 13) after re-entry in August 1999, almost 9 months after the well was initially suspended (Mobile North Sea Ltd 1999*a*). The DST perforated 100 m of the Clair Group from which the 6.5 m of 'oil-bubbling' core had been recovered the previous year (Fig. 13). The DST produced only water and did not flow oil to surface, with no technical issues reported during the DST (The Expro Group 1999).

213/23-1 (Eriboll) – Devonian

The Devonian Lower Clair Group (interpreted post-drill as Upper–Middle Old Red Sandstone: Fig. 13) is described as a fine- to coarse-grained, moderately sorted sandstone with poor porosity and poor oil shows within the end of well report (Mobil North Sea Ltd 1999*a*). No image logs were obtained within the Devonian interval of 213/23-1 (Eriboll) (Fig. 13). The average petrophysical properties throughout the Devonian section are shown in Table 3.

Post-drill interpretation of wireline data by Mobil suggested that a significant oil column was present in the Devonian–Carboniferous sequences, with average net-to-gross (NTG) of 42% and high water saturation (S_w) of 71% (Mobil North Sea Ltd 1999*a*, p. 7).

214/21a-2 (South Uist)

Well 214/21a-1 was drilled as part of a licence commitment in February 2008 by Shell and partners to target the South Uist gas prospect, located along an elongated (*c.* 4 km by 10 km) four-way dip-closed structure, around 10 km from the Corona Ridge structural high (Shell UK Ltd 2010). Pre-drill in-place estimates were 2.1 tcf (trillion cubic feet of gas) (Shell UK Ltd 2014). After extended operational challenges (e.g. blowout preventer (BOP) repairs and waiting on weather) the well was suspended and re-drilled as 214/21a-2 (South Uist) in July 2009 (Shell UK Ltd 2010). Before drilling, prognosed risks and uncertainties were the absence of reservoir and the age of the target interval, which was debated

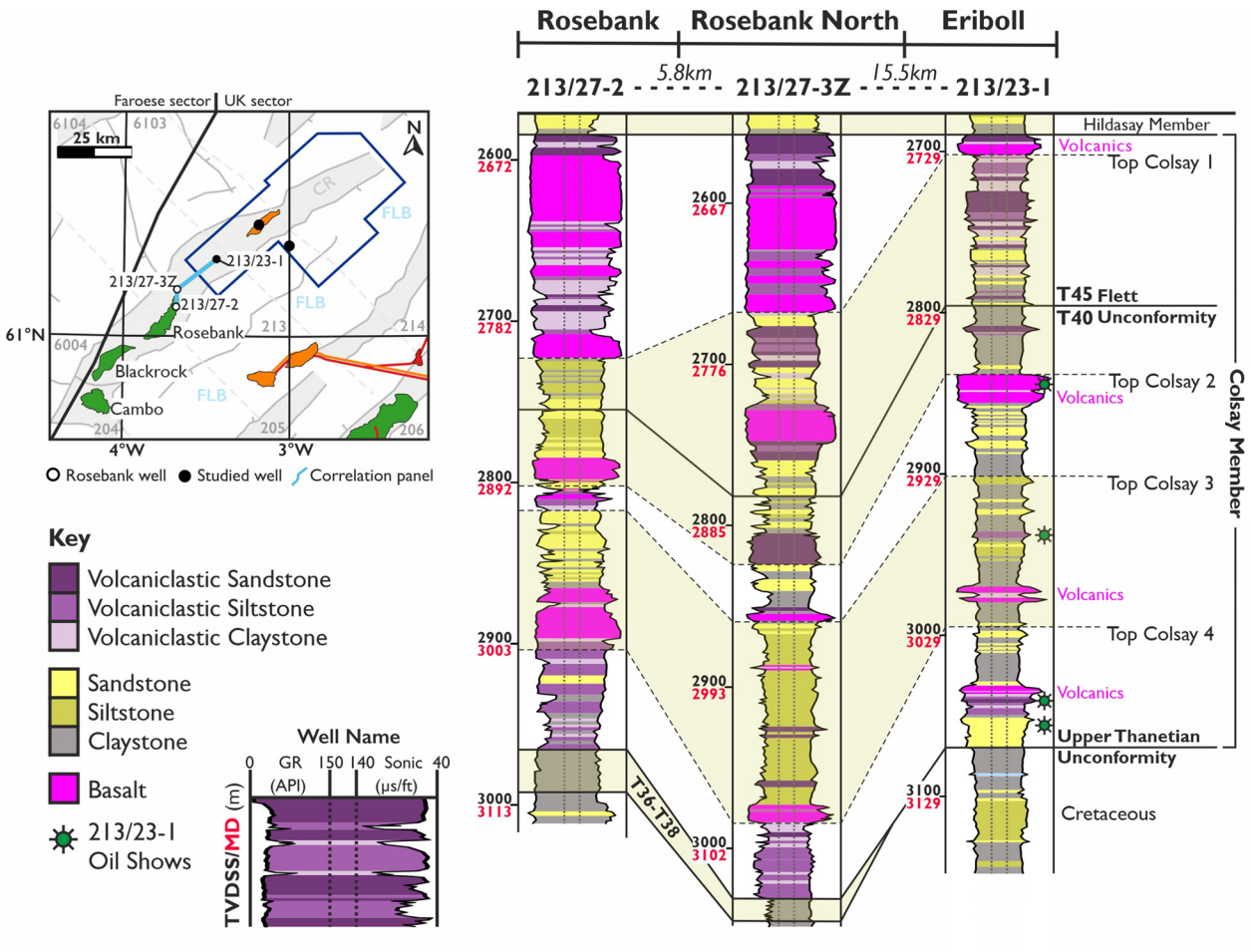

Fig. 11. Lithostratigraphic and sequence correlation of the T40–T45 Colsay Member (Colsay 1–4 units) from the Rosebank appraisal well 213/27-2 through the Rosebank exploration well 213/27-3Z and along the central-northern Corona Ridge into 213/23-1 (Eriboll). The main reservoirs within the Rosebank Field area are within the Colsay 1 and Colsay 3 intervals (Duncan *et al.* 2020). Note: the Upper Thanetian Unconformity (UTU) marks the top of sequence T38 (Fig. 4) (see Jolley *et al.* 2021).

by the well partners. Shell interpreted the target interval as the lower Paleocene Sullom Formation (T20); however, partner ConocoPhillips interpreted the target as Maastrichtian-age Cretaceous sedimentary rocks (Shell UK Ltd 2010). On drilling, the Sullom T20 target was encountered 173 m above the prognosed target depth. The target interval (>3713 m MD) consisted of Cretaceous mudstone and limestone stringers with no sandstones present, proving the stratigraphic interpretation of ConocoPhillips to be correct (Shell UK Ltd 2010).

213/25c-1V (North Uist)

213/25c-1V was drilled by BP over 295 days from March 2012 to January 2013, 12 km NW of South Uist, to fulfill licence commitments agreed with the regulator. The well was designed to test the Devonian–Carboniferous and/or Jurassic North Uist oil prospect estimated to contain 1067 MMboe in place (pre-drill P_{50} case: CNOOC Ltd 2017) within a three-way tilted fault block sealed by Jurassic and Cretaceous mudstones, with the reservoir prognosed at 4057 m MD (BP Exploration Operating Company Ltd 2013*b*). A secondary stratigraphic Paleocene target, the 430 MMboe in-place (pre-drill P_{50} case: CNOOC Ltd 2017) Cardhu prospect, was prognosed to lie beneath the Balder Formation at 3062 m MD (BP Exploration Operating Company Ltd 2013*c*). Operational challenges were encountered whilst drilling the well (see Watson *et al.* 2019), contributing to a rig mobilization of 312 days and costs estimated at more than £100 million (Energy Voice 2012; BP Exploration Operating Company Ltd 2013*b*). The well proved the presence of condensate within the Carboniferous Upper Clair Group and encountered Eocene–Devonian strata, including rocks of early–middle Jurassic age, before terminating at 4776 m MD within Devonian strata.

213/25c-1V (North Uist) – Paleocene–Eocene

The T60 middle Eocene Stronsay Group comprises mudstone with massive (*c.* 50 m-thick) interbeds of sandstone. Beneath the Stronsay Group, the Balder Formation was encountered, and is described as tuffaceous mudstone with siltstones, trace sandstone and trace limestone within the end of well report (BP Exploration Operating Company Ltd 2013*b*). Although not prognosed, an 8 m-thick (subseismic resolution) section of the Flett Formation was encountered within the secondary target (Cardhu) interval beneath the Balder Formation. Within well 213/25c-1V (North Uist), the Flett Formation is described as predominantly mudstone, with traces of sandstone observed as rock flour in cuttings. Although also not prognosed, the Lamba and Vaila formations were both penetrated below the Flett Formation (BP Exploration Operating Company Ltd 2013*a*). The Vaila Formation lies unconformably on the Upper Cretaceous Shetland Group.

213/25c-1V (North Uist) – Cretaceous and Jurassic

According to the composite log, the Upper Cretaceous strata consist of mudstone, siltstones and occasional limestone stringers (BP Exploration Operating Company Ltd 2013*a*). In well 213/

Table 2. *Descriptions of the Colsay Member (T40–T45) units 1–4 within the Rosebank Field (Hardman et al. 2018; Duncan et al. 2020) and 213/23-1 (Eriboll) (Mobil North Sea Ltd 1998, 1999c)*

Colsay unit	Rosebank Field	213/23-1 (Eriboll)
1	Siliciclastic successions of interbedded sandstones, siltstones and claystones with occasional volcaniclastic claystones and sandstones. Average gross thickness across the field is *c*. 56 m. Reservoir sandstones are described as very fine to medium grained (rarely coarse), sub-rounded to sub-angular, poorly cemented and moderately to well sorted with average porosities of 21–23%. Interpreted as braided fluvial sandstones within the T40 Colsay 1 interval and fully marine within the T45 Colsay 1 interval.	Siliciclastic and volcaniclastic sandstones, siltstones and claystones. Sandstones are very fine to medium grained, angular to sub-rounded, poor to well sorted, grain supported, friable, with occasional calcareous cement. Highest point-counted porosities seen are 15% with others as low as 5%. Reservoir quality is considered poor, reflecting high proportions of clay matrix, calcite cement and grain compaction. 10 m of T45 Colsay 1 core (Fig. 10) contains flat to low-angle lamination, wave-ripple lamination with local hummocky cross-stratification, bivalves, burrows and plant fragments interpreted as shallow-marine shelf deposits.
2	Thin siltstones, lignitic material and occasional volcaniclastic lithologies (siltstones and sandstones). Sandstones are described as fine (rarely coarse), well sorted and angular with visible porosities described as poor to moderate.	Sandstones, claystones and volcaniclastic claystone. Sandstones are very fine to medium (locally coarse), sub-rounded to rounded, moderately sorted and friable with intermediate porosities.
3	Successions of sandstones, claystones and siltstones with influxes of volcaniclastic sandstone indicative of an estuarine environment, overlain by fluvial sediments sourced from the SW. Average gross thickness across the field is *c*. 28 m. Reservoir sandstones are very fine to fine grained, occasionally coarse, sub-angular to angular, well sorted and poorly cemented with average porosities between 21 and 23%.	Sandstones, siltstones, claystones and volcaniclastic rocks (siltstone and claystone). Sandstones are very fine to fine, sub-angular to sub-rounded, moderately to poorly sorted, friable, very micaceous and grain supported with no visible matrix or cement present and poor porosity. One residual oil show was observed within volcaniclastic siltstone at *c*. 2955 m MD (Fig. 10). Porosities of sandstone cuttings are described as intermediate to poor; no values are given.
4	Interbedded clastic and volcaniclastic claystones and siltstones, interpreted as prodelta deposits. Average gross thickness of *c*. 22.5 m across the field. Sandstones are described as very fine, sub-angular to angular, well sorted and thin.	Sandstones, claystones and volcaniclastic lithologies (sandstone, siltstone and claystone). Sandstones are very fine to fine grained, sub-angular, moderately sorted, grain supported, with occasional calcareous cement and oil shows. Oil show observed (3079 m MD) within a 25 m-thick, friable, very fine to fine, sub-angular, moderately sorted reworked sandstone with 'loose' quartz grains.

Porosities given for Colsay units 1 and 3 within 213/23-1 are based on petrography of Colsay 1 core (Fig. 10) (Mobil North Sea Ltd 1999*c*) and Colsay 3 cuttings (Mobil North Sea Ltd 1999*a*). Porosities given for Colsay units 1 and 3 within the Rosebank Field are average porosity ranges from Duncan *et al.* (2020). Visible porosities for Colsay 2 within the Rosebank Field are based on Rosebank exploration and appraisal wells 213/26-1 and 213/27-3Z (Chevron Upstream Europe 2007*b*; 2009).

25c-1V (North Uist), oil shows were observed solely within cuttings from the Santonian Shetland Group at 3460 m MD. The section containing oil shows was drilled with oil-based mud (OBM) and, as oil show fluorescence is similar to that of the OBM fluorescence, shows were inconclusive. Lower Cretaceous strata are characterized by mudstone with limestone stringers and thin sandstones. The Lower Cretaceous lies unconformably on Lower–Middle Jurassic strata. Jurassic strata are characterized by organic-rich mudstones. The 68.8 m-thick Jurassic section lies unconformably on the Carboniferous Upper Clair Group (UCG).

213/25c-1V (North Uist) – Devonian–Carboniferous

Within the composite log, the Carboniferous UCG is characterized by sandstones with mudstone interbeds (BP Exploration Operating Company Ltd 2013*a*). The lower, Devonian–Carboniferous, section of the Clair Group comprises sandstone, siltstone and thin mudstones. Sedimentological observations of the Devonian–Carboniferous Clair Group are comparable to well 213/23-1 (Eriboll), suggesting a fluvial depositional environment, although this is speculative due to the lack of conventional (continuous) core obtained in 213/25c-1V (North Uist).

213/25c-1V (North Uist) discovered gas condensate (42.5° API: CNOOC Ltd 2017) in two reservoirs: the upper (Carboniferous, 3974–4069 m MD) and lower (referred to as Devonian–Carboniferous within the end of well report, 4069–4773 m MD) Clair Group reservoirs (Fig. 9b). No gas–water contact (GWC) was identified in the composite log or the end of well report, although neutron-density crossover implies a GWC at *c*. 4630 m MD. The much thicker (704 m) lower reservoir is referred to as 'tight', with very low mobilities (<0.1 mD/cP) suggestive of low permeabilities, which alongside high S_w (82%) resulted in no net pay interpreted by BP within the lower reservoir. Properties of the upper and lower reservoirs are shown in Table 3.

After drilling, the upper reservoir (North Uist discovery) was estimated to contain 104 MMboe (P_{50} case) of condensate in place, just under 10% of the pre-drill in-place P_{50} estimates (1067 MMboe) (CNOOC Ltd 2017). No well testing was performed, and the well was plugged and abandoned.

Seismic interpretation along the central-northern Corona Ridge

Top Crystalline Basement time–structure maps (Fig. 14) show the central-northern Corona Ridge as one structurally high (at *c*. 5 s depth TWT) feature within the SW of the study area, which splits into two structural highs towards the NE that have less relief (*c*. 6 s depth TWT). The southerly branch splits further into two components, creating a series of lows between the highs of crystalline basement within the NE of the dataset (Fig. 14b). The Corona Ridge is bound by a series of mapped normal faults that strike NE–SW (collectively termed the Flett-Corona Fault: Rippington *et al.* 2015) within the Flett Sub-basin. Two faults that strike north–south and NNW–SSE (red faults, Figs 5 and 14), oblique to the main series of NE–SW-striking faults (Fig. 14), are mapped within the centre of the dataset, where the Corona Ridge bifurcates. The time–structure map of the Top Crystalline Basement (Fig. 14) horizon clearly shows that the structure of the Corona Ridge is far more complex than previous interpretations (see Fig. 14b for comparison). Downflank fault terraces of Jurassic and/or Devonian–Carboniferous strata (Figs 7, 15a and 16a) were also identified, downthrown from the main Corona Ridge structure along the Flett–Corona Fault, which are overlain by Cretaceous and/or Jurassic sedimentary rocks.

Towards the base of the seismic survey (between 7 and 9 s TWT) a series of high-amplitude, hard (negative amplitudes/troughs

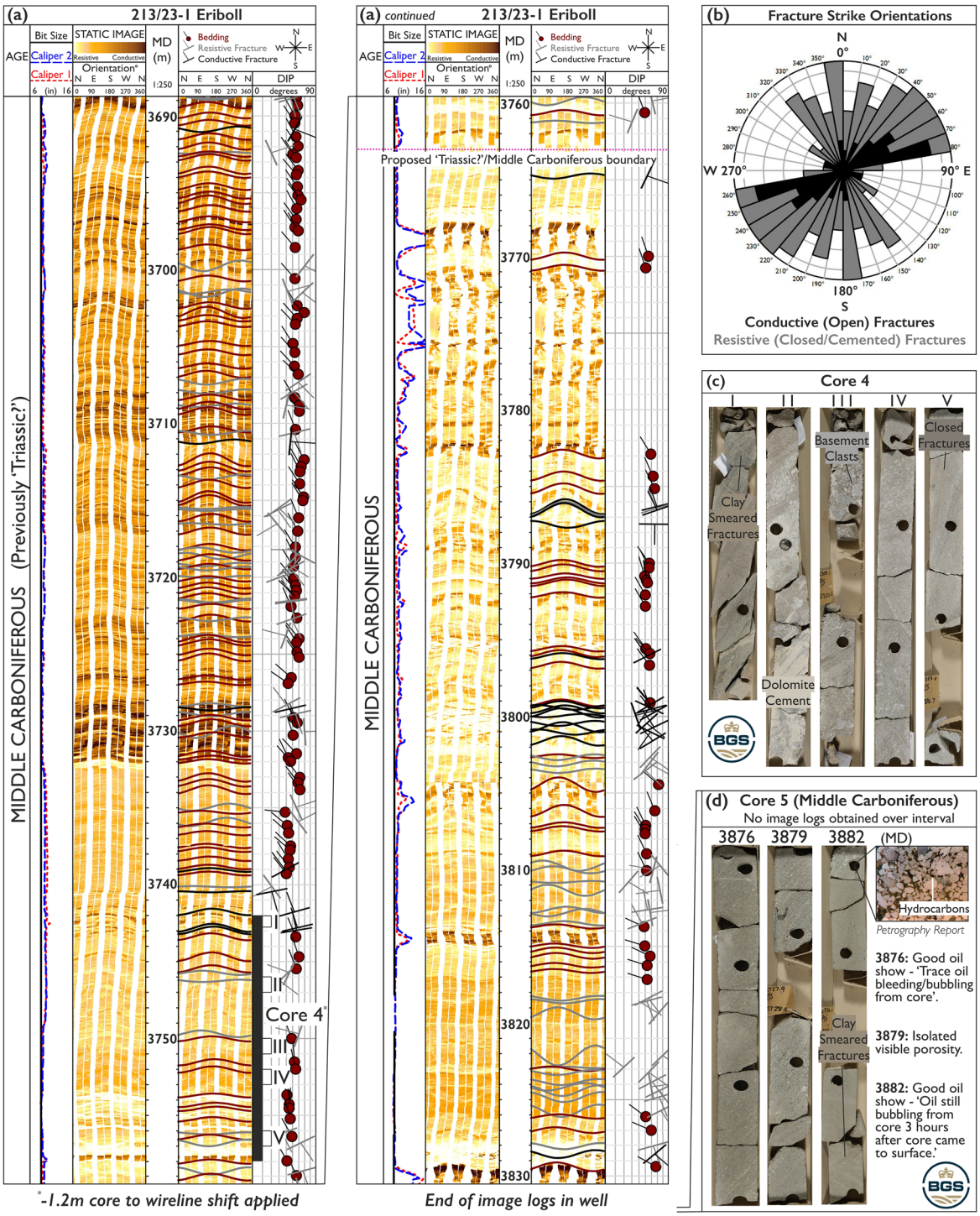

Fig. 12. (**a**) Resistivity image logs through the proposed 'Triassic?' (reinterpreted by this study as middle Carboniferous) and middle Carboniferous sections from 3689 to 3831 m MD within 213/23-1, with bedding sinusoids, resistive and conductive fractures, and their corresponding tadpole plot. Note: a structural dip of 55° has not been removed and locations of core 4 have been depth-shifted based on a −1.2 m core to wireline shift (Mobil North Sea Ltd 1999*d*). (**b**) Rose diagram showing the strike of resistive and conducive fractures interpreted within the section shown in (a). (**c**) Various photographs of core 4 obtained within the middle Carboniferous (previously interpreted post-drill as 'Triassic?'); locations of where core 4 was recovered are shown within (a). (**d**) Various photographs of core 5 obtained within the middle Carboniferous interval with key descriptions and an example of core petrography (Mobil North Sea Ltd 1999*c*) showing hydrocarbons present within pores. Note: no image logs were obtained over the core 5 interval, which was obtained from a deeper middle Carboniferous section. Core photographs are from British Geological Survey (2021).

displayed as red reflections on Fig. 5a), semi-continuous reflections (Fig. 5) can be observed beneath the central-northern Corona Ridge (labelled in Figs 5 and 7). The high-amplitude reflections appear to coalesce and have upwards concave geometries. The high-amplitude reflections are present at these depths throughout most of the 3D survey, although a much higher quantity is present in the centre of the 3D seismic dataset (e.g. Fig. 5) compared with the northern part of the dataset where there are none (Fig. 8). Assuming velocities based on Rippington *et al.* (2015) for the crystalline continental crust, this would place these reflections at depths of *c.* 16–20 km. The minimum vertical resolution at *c.* 18 km depth (*c.* 8 s TWT) is *c.* 270 m.

Based on our mapping of the Faroe–Shetland Sill Complex, emplacement of magma into Cretaceous and lower Paleocene sedimentary host rocks was generally confined to the Flett and Sissal sub-basins (Fig. 17). Only two igneous intrusions were interpreted within the seismic data to have been emplaced within the Cretaceous host rock directly above the central-northern Corona Ridge (Figs 5 and 17), implying a lack of magma emplacement.

Discussion

Crystalline basement structure of the central-northern Corona Ridge

Whilst the crystalline basement rocks of the Rona Ridge have been extensively studied (due to the Clair Field and other basement plays: e.g. Bonter and Trice 2019; Holdsworth *et al.* 2019), the Corona Ridge has received much less attention, and currently there are no detailed crystalline basement maps published. Work along the Corona Ridge has largely focused on prospectivity within overlying strata (e.g. Paleocene–Eocene plays: Hardman *et al.* 2018; Duncan *et al.* 2020) and tends to adopt simplified structural maps of the Corona Ridge. The NE–SW-trending structure of the central-northern Corona Ridge mapped as part of this study (Fig. 14b) shows that its structure is more complex than the older, poor, sub-basaltic seismic imaging previously allowed authors to image (e.g. Hughes *et al.* 1997; Ellis *et al.* 2009). Previous interpretations show the structural high as one crystalline block within the study area (see map bottom right in Fig. 14b), whereas we show that the central-northern Corona Ridge splits into three structural highs towards the NE, creating a series of lows (mini-basins: Fig. 14a) between the highs of crystalline basement. We also show that the NE–SW-striking Corona Ridge bounding normal faults (Fig. 14), often simplified as one feature within regional maps of the basin (e.g. Mudge and Rashid 1987; BGS 1996; Ellis *et al.* 2009; Ritchie *et al.* 2011) and collectively termed the Flett–Corona Fault by Rippington *et al.* (2015), in fact constitute a series of discrete faults that instead should be termed the Flett–Corona Fault System.

Oblique faults and downflank terraces of the Corona Ridge

The two north–south- and NNW–SSE-striking faults (red faults in Figs 5, 14 and 15a) mapped within the centre of the study area are oblique to the NE–SW-strike of basement bounding faults of the collectively termed Flett–Corona Fault System. The 'oblique' faults are expressed at both the Top Crystalline Basement and Base Cretaceous levels (red faults in Figs 5, 14 and 15a), and are located where the Corona Ridge is interpreted to bifurcate into two parts mapped within the NW of the dataset. Although much of the NE–SW-striking structural fabric in the FSB (and, indeed, broader NE Atlantic margin) is thought to reflect inheritance from pre-existing crystalline basement trends, the north–south-striking oblique faults do not appear to reflect structural inheritance from NW–SE-trending Precambrian shear zones (Knott *et al.* 1993), NE–SW-striking Caledonian compressional fault systems (Doré *et al.* 1997) or NW–SE-trending lineaments or 'transfer zones' (Rumph *et al.* 1993; Moy and Imber 2009). Dean *et al.* (1999) also mapped two dominant fault trends on the Corona Ridge (at the Base Cretaceous level, referred to as Base Upper Cretaceous in Dean *et al.* 1999), with north–south- and NE–SW-striking orientations, and postulated that the north–south faults were Jurassic in age. Obliquity of the north–south- and NNW–SSE-striking faults from dominant NE–SW-striking structural fabrics is also observed across parts of the NE Atlantic margin, including the North Viking Graben, Porcupine Basin and Møre Margin (Doré *et al.* 1997; Schiffer *et al.* 2020).

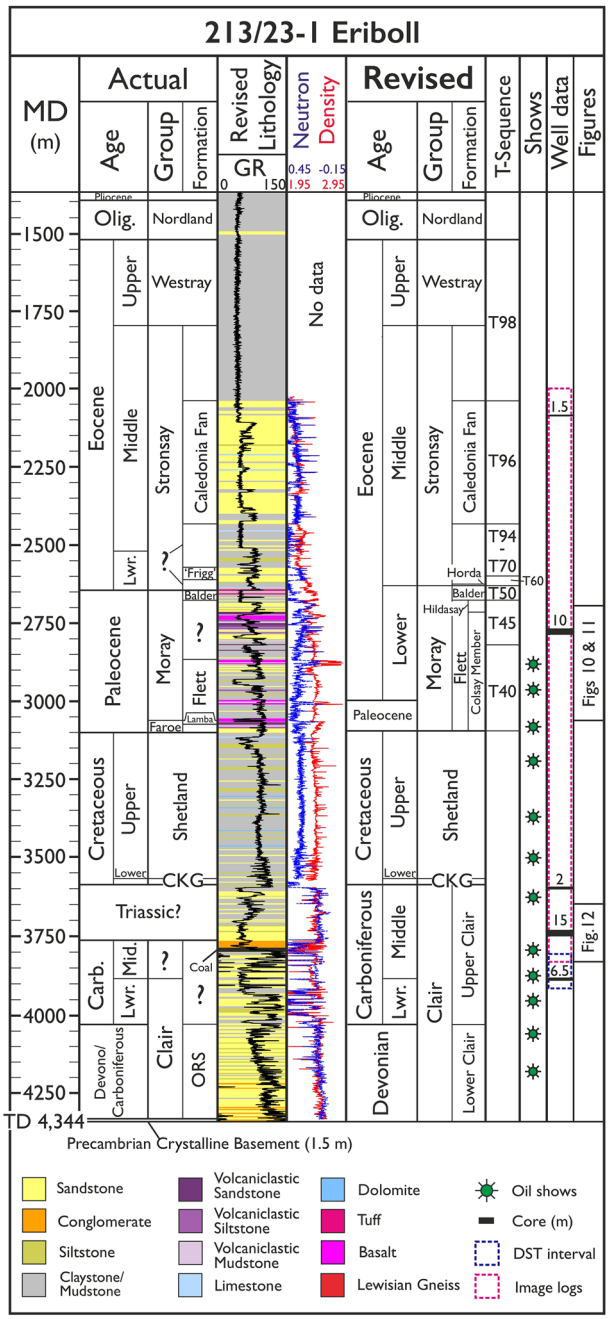

Fig. 13. Original post-drill stratigraphy (left: see also Fig. 9a, taken directly from Mobil North Sea Ltd 1999*a*) and reinterpreted (revised by this study) stratigraphy and lithology (reinterpreted for the Colsay Member) of well 213/23-1, with gamma-ray (GR) and neutron-density wireline logs, and relevant location of figures contributing to the reinterpretation of well 213/23-1 (Figs 10, 11 and 12). The Top Paleocene pick is based on the palynofloral stratigraphy by Jolley *et al.* (2021). Middle–upper Eocene T-sequence intervals are taken from Stoker *et al.* (2012). Note: (1) we interpret the Flett Formation to be 228 m thicker than interpreted post-drill (194 m); (2) our reinterpretation of the 'Triassic?' section is as a continuation of the underlying middle Carboniferous strata; (3) the section assigned 'Devono/Carboniferous' post-drill is now assigned to the Devonian; and (4) the Devonian–Carboniferous section has been split into the Lower and Upper Clair Group. Abbreviations; CKG, Cromer Knoll Group; ORS, Old Red Sandstone; TD, total depth; ?, undifferentiated.

North–south-striking rift basins within the NE Atlantic are thought to have originated either during east–west-directed Triassic–Jurassic extension, which exploited late Caledonian structures, or as a new trend established from northwards rift propagation during the early Cretaceous (Dean *et al.* 1999; Schiffer

Table 3. *Average petrophysical properties of the Carboniferous and Devonian intervals within wells 213/23-1 (Eriboll) and 213/25c-1V (North Uist) obtained from end of well reports (Mobil North Sea Ltd 1999a; BP Exploration Operating Company Ltd 2013b)*

	Carboniferous (*c.* 3585–4028 m MD)	Devonian (4028 m MD – TD)	Carboniferous Upper Reservoir (3974–4069 m MD)	Devonian–Carboniferous Lower Reservoir (4069–4773 m MD)
213/23-1				
Porosity (%)	15	13		
Net-to-gross (NTG)	0.52	0.22		
Water saturation (%)	68	77		
213/25c-1V				
Gross thickness (m)			94.5	704
Net pay (m)			32.2	566*
Porosity (%)			14	11
Net-to-gross (NTG)			0.34	0.80
Water saturation (%)			56	82

*BP interpret no net pay as due to high water saturations and a lack of successful pressure tests (BP Exploration Operating Company Ltd 2013*b*).

et al. 2020). It has also been suggested that the north–south structural trends seen across the NE Atlantic margin may reflect the reactivation of pre-Caledonian or Caledonian suture zones, although direct evidence for this is sparse (Schiffer *et al.* 2020). Assessing the origins of oblique faults mapped here (red faults in Figs 5, 14 and 15a) and any further extent of north–south-striking faulting across the FSB is challenging, as the imaging of basement structures are often obscured by overlying Paleogene lava flows and the Faroe–Shetland Sill Complex (Hardwick *et al.* 2010). However, the identification of north–south structuration within the crystalline basement of the central-northern Corona Ridge suggests that such features could be more extensive than previously realized within the basin.

Downflank fault terraces of Jurassic and/or Devonian–Carboniferous strata (Figs 7, 15a and 16a) overlain by Cretaceous and/or Jurassic sedimentary rocks were also identified downthrown from the main Corona Ridge structure along the Flett–Corona Fault System. Barr *et al.* (2007) described several similar terraces that extend the Clair Field from the main Rona Ridge structure, which also comprises Devonian and Jurassic strata (referred to as the Clair South development: Robertson *et al.* 2020).

High-amplitude reflections beneath the central-northern Corona Ridge

A series of hard (negative amplitudes/troughs displayed as red reflections on Fig. 5a) high-amplitude reflections are observed within the 3D seismic data (Figs 5 and 7) beneath the central-northern Corona Ridge between 7 and 9 s TWT (*c.* 16–20 km depth). The high-amplitude reflections have upward-concave geometries and often appear to coalesce with other high-amplitude reflections. The minimum vertical resolution at *c.* 18 km depth (*c.* 8 s TWT) is *c.* 270 m. Seismic refraction data and associated velocity modelling within the study area (e.g. iSIMM, Mobil-1 and Mobil-2 lines: White *et al.* 2005; Makris *et al.* 2009; Roberts *et al.* 2009) indicate that the depth to the Moho beneath the Corona Ridge is *c.* 17–20 km (Funck *et al.* 2017; Petersen and Funck 2017). It is therefore likely that the high-amplitude reflections are located within the lower crust.

Whilst there is no direct evidence as to the origin of these high-amplitude reflections, through comparison with analogous high-amplitude reflections published throughout the NE Atlantic margin that have the same reflectivity, geometries and are located at similar depths (*c.* 15 km, White *et al.* 2008; *c.* 7–9 s TWT, Abdelmalak *et al.* 2017 and Wrona *et al.* 2019), we tentatively propose that the high-amplitude reflections could be caused by basic intrusive bodies within the lower crust.

Devonian–Carboniferous Clair Group

The Clair Field, located on the Rona Ridge (*c.* 70 km from the central Corona Ridge), is expected to produce over 940 MMbo (million barrels of oil) from Devonian–Carboniferous Clair Group reservoirs (Robertson *et al.* 2020). The discovery of 104 MMboe in place (post-drill P_{50} case) of condensate in North Uist (213/25c-1V) proves that the Devonian–Carboniferous is a working play on the Corona Ridge (CNOOC Ltd 2017). However, no well tests were performed within well 213/25c-1V, which limits the interpretation of the reservoir volume and accurate estimation of the post-drill connected in-place volume of North Uist.

Remnants of an intermontane basin are mapped on the Corona Ridge (Fig. 14b) that contain Devonian–Carboniferous strata penetrated by wells 213/23-1 (Eriboll) and 213/25c-1V (North Uist) (Fig. 16a). We also note the presence of the Clair Group below the Rosebank Field to the SW of the study area, confirmed by wells 213/27-1Z (95.8 m) and 213/27-2 (90 m) (Fig. 1b) (ChevronTexaco Upstream Europe 2004; Chevron Upstream Europe 2007*a*). The intermontane basin possibly present along the Corona Ridge throughout the Devonian–Carboniferous is perhaps analogous to the Clair Basin located on the Rona Ridge (Ritchie *et al.* 2011; Smith and Ziska 2011). No Devonian–Carboniferous Clair Group was reported to have been penetrated to the NE of the study area in well 214/09-1 (Bunnehaven: Fig. 1b), and hence most previous work (e.g. Smith and Ziska 2011; Stoker *et al.* 2014) does not extend its distribution north of 213/25c-1V (North Uist). Smith and Ziska (2011) interpreted 213/23-1 (Eriboll) as the only well to penetrate the entire Devonian–Carboniferous sequence on the Corona Ridge (totalling 753 m) before terminating in crystalline basement. The lack of penetrations of the entire Devonian–Carboniferous sequence on the Corona Ridge compared with the Rona Ridge does not allow for comparison of thicknesses across the two ridges. However, our mapping of the thickness of the Devonian–Carboniferous sequences (Fig. 16a) does reflect varying thicknesses of the Devonian–Carboniferous strata (0–1.6 s TWT), comparable to the variable thicknesses within the Clair Field (*c.* 150–900 m: Robertson *et al.* 2020) and the Rona Ridge as a whole (*c.* 1000 m: Ziska and Anderson 2005).

Early Clair Field wells (drilled from 1977 to 1985) failed to confirm economical amounts of recoverable hydrocarbons within the Clair Group on the Rona Ridge (Robertson *et al.* 2020). Ogilvie *et al.* (2015) attributed the low flow rates (<1000 bopd (barrels of oil per day)) observed in early appraisal drilling to vertical wells being unlikely to penetrate potentially productive open fractures, compared with later-stage horizontal well sections (i.e. during the 1990s) that penetrated vertical fractures, proving that required flow

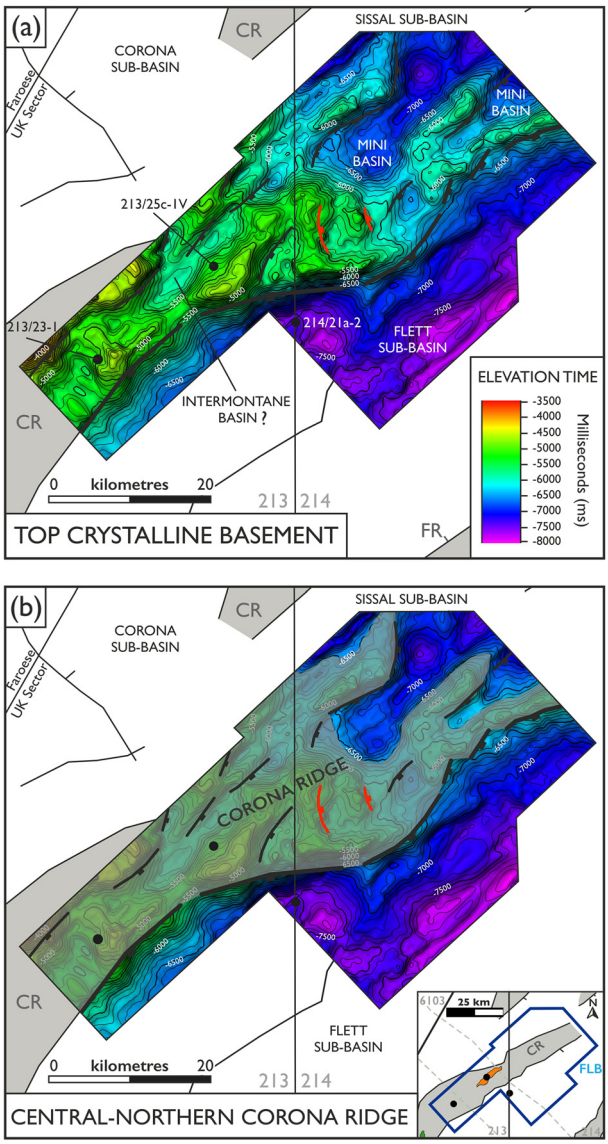

Fig. 14. (**a**) Top Crystalline Basement surface time–structure map including structural elements mapped; note the presence of oblique faults (in red) trending north–south and NNW–SSE. Also see Figure 5 for seismic data through the oblique faults. (**b**) Top Crystalline Basement surface time–structure map and structural elements (a) showing the area of the central-northern Corona Ridge (transparent grey) considered by this study (as defined by Peacock and Banks 2020). Note: (1) the series of lows (mini-basins) between the sections of crystalline basement within the NE of the dataset; (2) possible remnants of an intermontane basin labelled on the Corona Ridge; and (3) the small map (b, bottom right) showing the previous interpretation of the Corona Ridge taken from Figure 1 (Ellis *et al.* 2009).

rates could be achieved. We note that well 213/23-1 (Eriboll), much like early Clair Field appraisal wells, had a vertical trajectory and was therefore not orientated optimally to intersect any open fracture sets that may be present. The DST performed within 213/23-1 (Eriboll) also tested only 100 m of lower–middle Carboniferous strata, which is 10% of the length which was needed to obtain successful flow rates (18 000 bopd) from a 950 m horizontal section within the later-stage Clair Field appraisal wells (206/8-10 and 206/8-10z: Fig. 1b) (Robertson *et al.* 2020). Core obtained within the tested interval of 213/23-1 (Eriboll) (Fig. 12c) exhibits evidence of abundant calcite cementation and is not representative of the 753 m-thick Devonian–Carboniferous section that showed positive early signs of oil present (3876–3884 m MD: e.g. positive flow tests and oil shows 'bubbling' from core). We therefore suggest that Eriboll may be under appraised.

Devonian–Carboniferous Clair Group: is there fracture enhanced permeability along the central-northern Corona Ridge?

According to critical stress theory, fractures optimally orientated in relation to the present-day stress field (usually parallel to the orientation of $S_{H\,max}$) are more likely to be hydraulically conductive and thus potentially allow the transmission of fluids (Hillis 1997; Rogers 2003; Tassone *et al.* 2017). On the central-northern Corona Ridge, we interpret an $S_{H\,max}$ orientation of NW–SE, which is consistent with general trends of present-day maximum horizontal stress observed across NW Europe (Holford *et al.* 2015). Therefore, according to critical stress theory, NE–SW- and ENE-WSW-striking Carboniferous fractures that we interpret within 213/23-1 (Eriboll) (Fig. 12) are not optimally orientated for enhanced fracture permeability, much like the Carboniferous strata of the Clair Field on the Rona Ridge (Robertson *et al.* 2020).

Within the Devonian Lower Clair Group reservoir of the Clair Field, according to Robertson *et al.* (2020), enhanced fracture permeability has been instrumental in achieving commercial flow rates. In contrast to the Clair Field, only poor oil shows were encountered within the Devonian strata penetrated by well 213/23-1 (Eriboll), and subsequently no image logs were obtained and no DST was completed within the Devonian section of 213/23-1, which precludes the analysis of any potential fracture permeability that may be present within Devonian strata along the central-northern Corona Ridge.

Absence of Triassic on the Corona Ridge: extending the Devonian–Carboniferous play

Less than 2 years after Mobil drilled well 213/23-1 (Eriboll) in 1998, ExxonMobil drilled well 214/09-1 (Bunnehaven: Fig. 1b) 92 km to the NE along the Corona Ridge, continuing to chase the 'pre-rift' section. No Devonian–Carboniferous strata were reportedly penetrated within 214/09-1 (Bunnehaven), although the well penetrated a 73 m-thick 'indeterminate' interval unconformably overlying Lewisian Crystalline Basement, which, like the proposed 'Triassic?' interval in 213/23-1 (Eriboll), was barren of *in situ* microfossils (ExxonMobil 2001). The indeterminate interval within 214/09-1 (Bunnehaven) was characterized by claystones, sandstones, dolomite and gneissic conglomerates, comparable to the interval reinterpreted as middle Carboniferous within 213/23-1 (Eriboll) previously assigned as 'Triassic?' (see Fig. 12c, core 4) (ExxonMobil 2001). The nearest Triassic penetration to the Corona Ridge is 80 km away, to the SE on the Rona Ridge (206/05-2: Fig. 1b), with these strata described as red beds with reddish brown claystone and occasional fragments of hard limestone (Conoco (UK) Ltd 1996); none of these lithologies are described in either 213/23-1 (Eriboll) or 214/09-1 (Bunnehaven) (Fig. 1b).

Triassic strata in the FSB are typically entirely barren of all fossil groups (Swiecicki *et al.* 1995). According to Morton *et al.* (2010) and Morton and Milne (2012), the Devonian–Carboniferous strata of the Clair Field are also entirely barren, making age determination between Triassic and Devonian–Carboniferous sections challenging. Age determination of the Carboniferous UCG section in 213/25c-1V (North Uist) using biostratigraphic and heavy mineral data was also challenging according to the end of well report, comparable to the challenges associated with the proposed 'Triassic?' interval in 213/23-1 (Eriboll) and the indeterminate interval in 214/09-1 (Bunnehaven).

The distribution of Permian–Triassic rocks in the central FSB (e.g. Quinn and Ziska 2011; Stoker *et al.* 2014, 2017*b*) is inferred

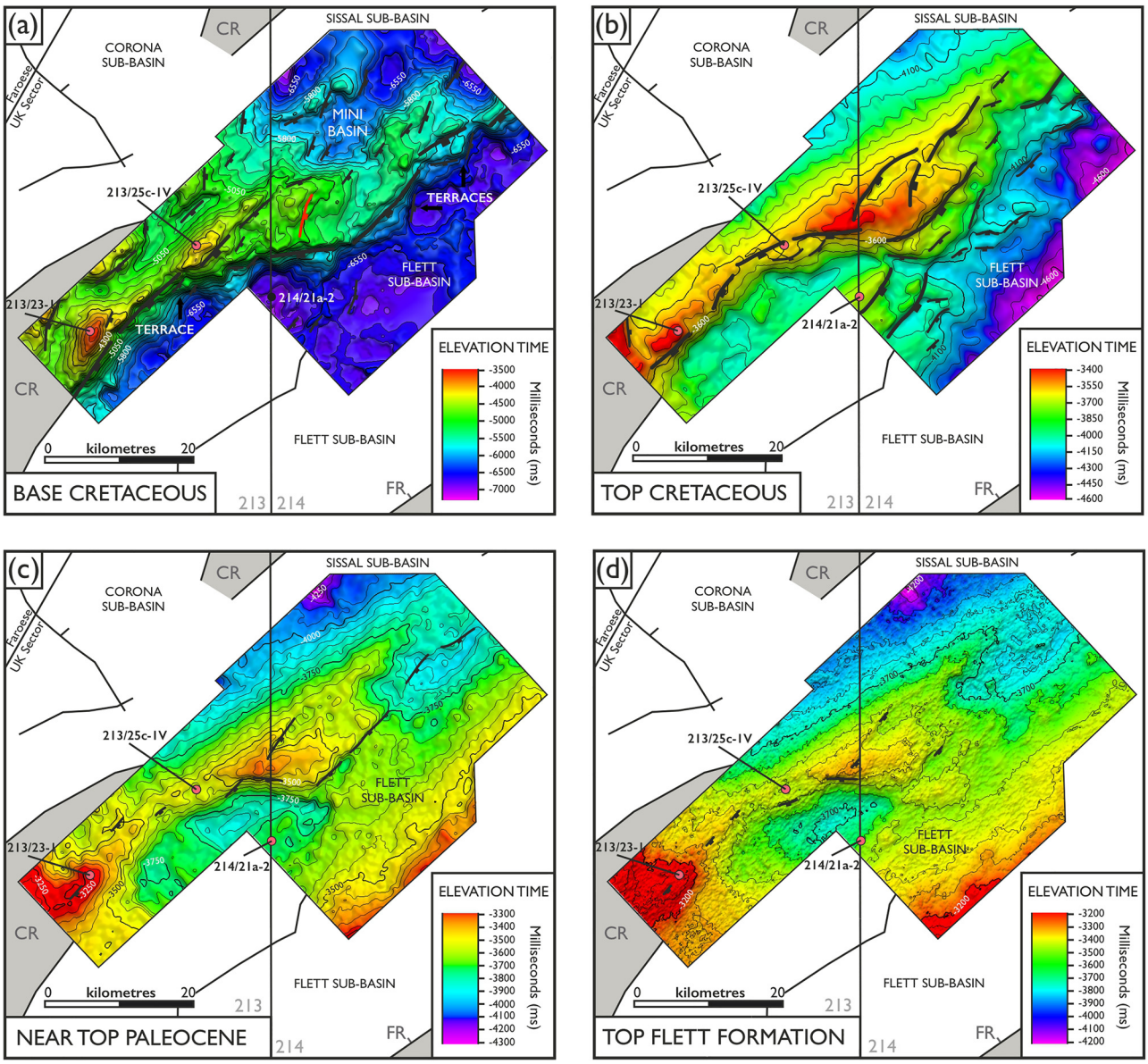

Fig. 15. Time surfaces with structural elements of (**a**) the base Cretaceous (oblique fault in red), (**b**) the Top Cretaceous, (**c**) the near Top Paleocene and (**d**) the Top Flett Formation within the study area. Note: (1) wells shown in red reflect where wells have penetrated the surface; (2) faults shown within the near Top Paleocene (c) and Top Flett Formation (d) are all minor faults and (3) the presence of the structures targeted by 213/23-1 (Eriboll) and 213/25c-1V (North Uist) in (a) and the structure targeted by 214/21a-2 (South Uist) in (b).

solely based upon two proposed well penetrations: 213/23-1 (Eriboll) and 214/09-1 (Bunnehaven) (Fig. 1b). Our interpretation of the absence of Triassic strata from 213/23-1 (Figs 12 and 13), alongside the absence of Triassic strata from other areas of the Corona Ridge (213/25c-1V, North Uist and 213/27-1Z, Rosebank), casts doubt on the interpretation of the presence of Triassic strata within 214/09-1 (Bunnehaven: Fig. 1b) (Quinn and Ziska 2011; Stoker *et al.* 2014, 2017*b*) and therefore from the central FSB, with penetrations of Triassic strata possibly confined solely to the present-day margins of the FSB within the Judd (204/29-1) Sub-basin and the Westray High (204/19-1 and 204/19-9) (Fig. 1b) (see Štolfová and Shannon 2009).

If, like 213/23-1 (Eriboll), the indeterminate interval in well 214/09-1 (Bunnehaven) is Devonian–Carboniferous in age and not Triassic (or Jurassic), this could provide renewed potential for the presence of exploration plays of this age (provided that there is Devonian enhanced fracture permeability and large enough structural closures) and the possible presence of gas-prone source rocks (Carboniferous coals: Figs 2 and 13) along the northern Corona Ridge, which have not previously been interpreted this far north (Quinn and Ziska 2011; Stoker *et al.* 2014, 2017*b*). This may also have wider implications in understanding the early geological evolution of the FSB subsequent to post-Caledonian orogenic collapse, as Devonian–Carboniferous depositional systems may have been far more extensive than previously thought within the north of the FSB (Stoker *et al.* 1993; Nichols 2005; Smith and Ziska 2011).

Our interpretation of no Triassic strata present within 213/23-1 suggests an unconformity between middle Carboniferous and Lower Cretaceous strata of at least 154 myr. Implications of our interpretation, the absence of Triassic strata, are that: either (1) Permian–Triassic rocks were deposited but then eroded from the Corona Ridge and recycled into the adjacent Corona, Flett and Sissal sub-basins as synrift reservoir units throughout the late Jurassic–early Cretaceous evolution of the Corona Ridge; or (2) no Permian–Triassic rocks were deposited as the Corona Ridge was a prominent structural high throughout the Permian–Triassic.

Although the interpretation of Permian–Triassic strata being eroded during the late Jurassic–early Cretaceous development of relief along the Corona Ridge (Ritchie *et al.* 2011; Hardman *et al.*

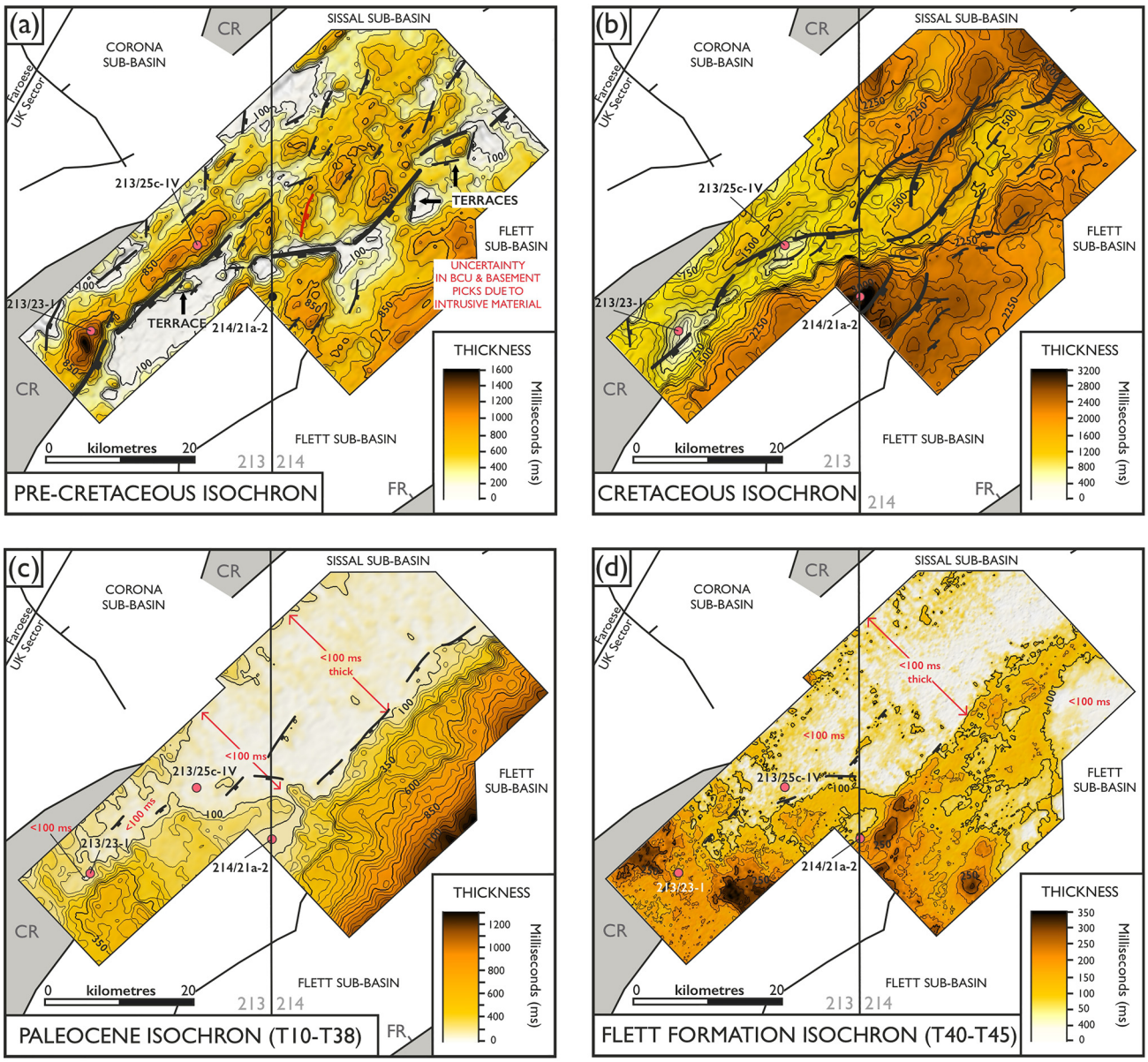

Fig. 16. Isochron time maps of (**a**) the pre-Cretaceous (Devonian–Carboniferous and Jurassic) based on Basement (Fig. 14a) to base Cretaceous (Fig. 15a), with relevant structural elements (oblique fault shown in dark red). Due to the absence (e.g. 213/23-1) and thin (e.g. 213/25c-1V) presence of Jurassic encountered on the central-northern Corona Ridge along the structural high, the isochron can be used to infer Devonian–Carboniferous thicknesses. Note: we interpret no Triassic present in the study area; (**b**) the Cretaceous, (**c**) the Paleocene and (**d**) the Flett Formation within the study area. Note: (1) wells shown in red reflect where wells have penetrated the interval; and (2) where thicknesses of both the Paleocene (c) and Flett Formation (d) are less than 100 ms, intervals may be absent (e.g. the Paleocene T10–T38 interval is absent in well 213/23-1).

2018) is supported by the lack of Permian–Jurassic strata within 213/23-1, the preservation of Lower–Middle Jurassic within 213/25c-1V (North Uist) and Upper Jurassic-age strata within 213/27-1Z does not support this interpretation (ChevronTexaco Upstream Europe 2004; BP Exploration Operating Company Ltd 2013*b*). If the latter interpretation is correct, the Corona Ridge may have been a structurally high feature during the Permian–Triassic (hence no deposition) which was then drowned during the proposed Jurassic marine incursion (Dean *et al.* 1999), and then re-emerged during the late Jurassic–early Cretaceous rift period, which is understood to be largely responsible for the present-day structure of the Corona Ridge (Ritchie *et al.* 2011; Hardman *et al.* 2018). During late Jurassic–early Cretaceous extension there may have been some localized shedding and recycling of Carboniferous and Jurassic strata from the Corona Ridge (forming localized synrift targets) into adjacent sub- and mini-basins (Figs 14 and 15a). This may explain the absence (in 213/23-1) and relatively thin (68.7 m in 213/25c-1V compared with 452 m penetrated in 213/27-3Z) presence of Jurassic strata along the central-northern Corona Ridge (Chevron Upstream Europe 2009; BP Exploration Operating Company Ltd 2013*b*).

The Lower Cretaceous synrift play

The possible recycling of 'pre-rift' Devonian–Carboniferous, Permian–Triassic and Jurassic strata from emergent structural highs (such as the Rona Ridge: Clark *et al.* 2020), with the addition of extrabasinal sediment (Stoker and Ziska 2011), during widespread early Cretaceous extensional deformation is thought to be responsible for the deposition of Lower Cretaceous reservoirs of the Cromer Knoll Group, which act as reservoirs for the Edradour Field and Glendronach discovery (Stoker 2016; Clark *et al.* 2020). Evidence of this widespread early Cretaceous extension can be observed within Figures 7 and 8, where synsedimentary deposition of Cretaceous sediments appears to relate to normal faults. Within the West Shetland

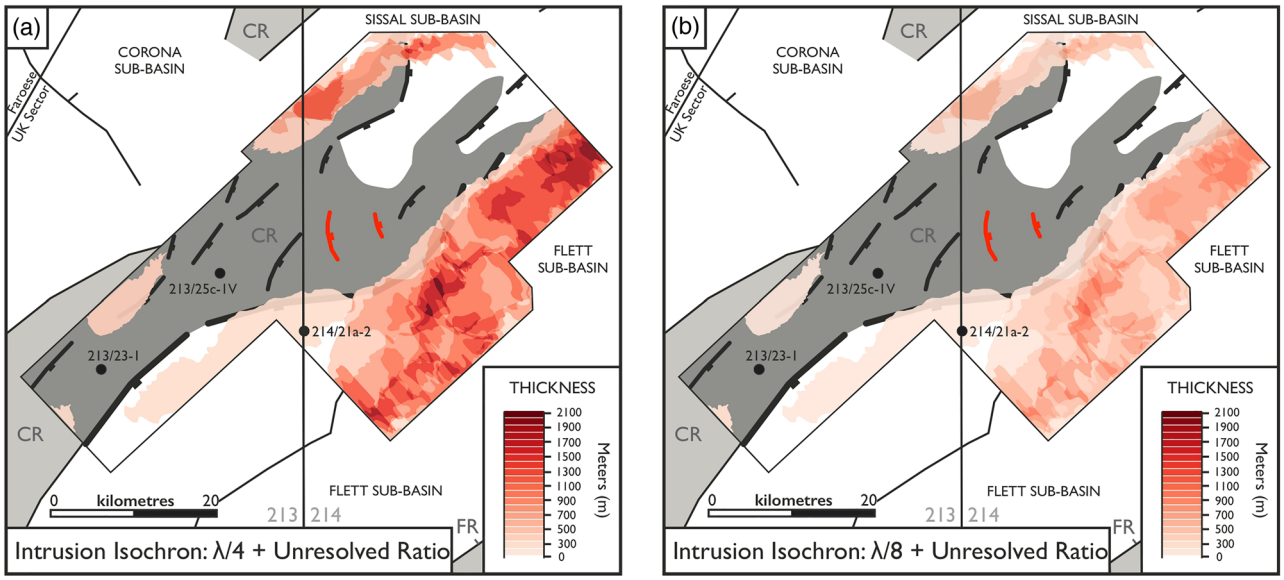

Fig. 17. Thickness maps of igneous intrusions emplaced within the Phanerozoic sedimentary sequences above the central-northern Corona Ridge showing (**a**) 1/4 wavelength thickness and (**b**) 1/8 wavelength thickness scenarios, both of which incorporate the ratio of 1:1.4 m of resolved:unresolved igneous material (see Mark *et al.* 2018*a*). The figure highlights the much thicker pile of intrusions within the Flett and Sissal sub-basins compared with the lack of emplacement into Phanerozoic sedimentary sequences overlying the central-northern Corona Ridge (CR). Note: (1) the grey structural elements outside of the study area are based on Figure 1 (Ellis *et al.* 2009); and (2) the dark grey area within the study area corresponds to the crystalline basement structure of the central-northern Corona Ridge (CR) interpreted by this study (see Fig. 14b).

Basin, the Lower Cretaceous Victory Formation is also a proven gas reservoir for the Victory Field (Figs 1b and 2) (Goodchild *et al.* 1999). Rift-related topography is thought to have controlled synrift depositional systems throughout the early Cretaceous along major relay ramps into inherited half-graben (Larsen *et al.* 2010).

Localized recycling of Carboniferous and Jurassic strata during the late Jurassic–early Cretaceous emergence of the Corona Ridge (as discussed in the previous subsection) is possibly reflected by the thin presence of the Lower Cretaceous Cromer Knoll Group within wells 213/23-1 (Eriboll: Fig. 9a), 213/25c-1V (North Uist: Fig. 9b) and 214/09-1 (Bunnehaven) (*c.* 120 m: ExxonMobil 2001), and the irregular occurrence of Jurassic rocks along the Corona Ridge (e.g. absent in 213/23-1 but present in 213/25c-1V and 214/09-1). Within neighbouring basins such as the Flett Sub-basin, into which localized shedding of eroded sediment may have occurred from the Corona Ridge, Lower Cretaceous intervals are much thicker, reaching up to 1168 m (Stoker 2016). The Cretaceous significantly thickens (>2000 ms) from the relief present along the central-northern Corona Ridge at the Base Cretaceous level (Figs 15a and b) into Cretaceous depocentres of the Sissal Sub-basin and other mini-basins identified between the sections of the Corona Ridge within the NE of the dataset (mini-basins: Fig. 14b). This suggests that there may be the potential for packages of Lower Cretaceous synrift plays to be present in the NE of the study area, with play fairways located off structural highs.

At the time of publication, no well has specifically targeted the Lower Cretaceous synrift play near the central-northern Corona Ridge within the sub-basins (Corona, Flett and Sissal) in and around the northern area of the FSB (Larsen *et al.* 2010; Stoker and Ziska 2011). In general, few wells have specifically targeted Lower Cretaceous strata in the northern FSB. Well 208/24-1A (NE part of the Flett Sub-basin: Fig. 1b) encountered 64.7 m of Lower Cretaceous sandstone that contained no oil shows (Stoker and Ziska 2011). Wells that have encountered Lower Cretaceous sands within the northern FSB whilst targeting other intervals are confined to the Corona Ridge (214/09-1, Bunnehaven) and the Erlend High (209/12-1) (Fig. 1b). Thin Lower Cretaceous sands encountered in both wells (214/09-1 and 209/12-1: Fig. 1b) were only observed as rock flour at the surface. The bias resulting from wells drilled upon structural highs restricts the understanding of how synrift Lower Cretaceous reservoirs may be distributed within the deeper sub-basin areas such as the Corona, Flett and Sissal sub-basins. The possible distribution of Lower Cretaceous reservoirs is therefore largely implied by underlying structures (Figs 14 and 15a), which may have influenced the deposition of synrift Cretaceous sediments into structural lows off the Corona Ridge within the NE of the study area.

Igneous intrusions emplaced within Cretaceous strata along the central-northern Corona Ridge

There is a lack of igneous intrusion emplacement within the Phanerozoic sedimentary sequences directly above the central-northern Corona Ridge itself (Fig. 17). This contrasts with the Flett Sub-basin where significant amounts of igneous intrusions have been emplaced within Cretaceous and lower Paleocene sedimentary rocks (Figs 7, 8 and 17). This possibly suggests that magma was less able to exploit the thick crust via basement-bounding faults (e.g. the Flett-Corona Fault System) during periods of Paleogene intrusive magmatism along the central-northern Corona Ridge, in comparison to the thinner crust of the basinal areas (Schofield *et al.* 2017).

Paleocene–Eocene: Colsay Member T40–T45 prospectivity

Distribution of sequences T40–T45 along the central-northern Corona Ridge

Since the discoveries of the Cambo (discovered 2002) and Rosebank (discovered 2004) fields, totalling *c.* 700 MMboe of recoverable resources, exploration and research focus has been largely confined to post-rift Paleocene–Eocene-aged reservoirs along the Corona Ridge (Smallwood and Kirk 2005; Austin *et al.* 2014; Loizou 2014; Siccar Point Energy 2020*a*). The Rosebank Field reservoir is within the upper Paleocene–lower Eocene-aged intra- and sub-basaltic Colsay Member (T40–T45) sandstones. During T40–T45 deposition of the Colsay Member a series of flood basalt (lava) sequences of the FIBG were also emplaced, forming

intra-basaltic stratigraphic plays along the Corona Ridge (Jolley and Bell 2002; Passey and Jolley 2009; Hardman *et al.* 2018).

Along the Cambo High and within the south Rosebank Field, the T40–T45 interval has a very distinct seismic response that is characterized by a series of stacked high-amplitude reflections (Poppitt *et al.* 2018, p. 378, fig. 6; Duncan *et al.* 2020, p. 985, fig. 6) that are tied to individual T40–T45 Colsay units (Hardman *et al.* 2018, p. 77, fig. 7a). Throughout most of the dataset used in this study, no similar Flett Formation seismic response is observed, except for the area south of 213/23-1 (Eriboll) (Fig. 5) which does not appear to correlate with areas containing the thickest presence of the Flett Formation (Fig. 16d).

Schofield and Jolley (2013) proposed that where a clastic intra-basaltic depositional system develops, lava-field morphology plays an important role in controlling and diverting sediment input, drainage systems and subsequent reservoir deposition within topographical lows in and around the margins of the lava fields. Understanding the structure present along the Corona Ridge (e.g. palaeohighs and lows underlying sequence T40) prior to (Fig. 15b) and during (Fig. 15c) the deposition of such complex sequences is also, according to Hardman *et al.* (2018), key to identifying sequence T40–T45 intra-basaltic play fairways within the central-northern Corona Ridge area. Our mapping of structures (Fig. 15) underlying such complex depositional systems and our identification of volcanic intervals previously missed within 213/23-1 (Eriboll) (Fig. 11) has facilitated a more detailed understanding of the possible distribution of T40–T45 intra- and sub-basaltic play fairways along the central-northern Corona Ridge. Sequence T40 intra-basaltic Colsay sediment is thought to have predominantly been deposited within topographical lows (Schofield and Jolley 2013) parallel to palaeohighs (NE–SW) present along the Corona Ridge, where drainage systems are thought to have developed (Hardman *et al.* 2018). This distribution of T40–T45 sediments is also reflected within our mapping (Figs 15 and 16). The NW–SE trend present within the T40–T45 isochron (Fig. 16d) runs parallel to the central-northern Corona Ridge and is thickest within the topographical lows present at the near Top Paleocene level (Fig. 15c). Significant thinning of the Flett Formation from 422 m within well 213/23-1 (Eriboll) to 8 m within 213/25c-1V (North Uist) (over 18 km: Fig. 16d) also reflects the complex distribution of sequence T40–T45 along the Corona Ridge discussed by Schofield and Jolley (2013). This is possibly attributed to the palaeohigh present to the north of 213/25c-1V (North Uist) at the Top Cretaceous (Fig. 15b) and near Top Paleocene levels (Fig. 15c) that may have acted to divert sediment into the topographical low adjacent to the central-northern Corona Ridge.

Although published research has largely overlooked the possible distribution of intra- and sub-basaltic Paleocene–Eocene-aged (sequence T40) reservoirs NE of the Rosebank Field, an examination of prospectivity by OMV and partners *c.* 50 km north of the study area, within now relinquished licence area P1997 (Fig. 1b), suggests that reservoir presence and quality is high risk within the Paleocene–Eocene Flett interval and that seismic imaging is too poor to allow calibration with offset wells (OMV 2015).

Extending the intra- and sub-basaltic plays of the Rosebank Field along the central-northern Corona Ridge

The reinterpretation of the Flett Formation within well 213/23-1 (Eriboll) has facilitated the identification of four volcanic intervals and intra-basaltic and sub-basaltic sandstones of the Colsay Member (sequence T40–T45). These intervals were not previously interpreted within 213/23-1 (Eriboll) (Mobil North Sea Ltd 1999*a*) and were not previously thought to extend this far north along the Corona Ridge from the Rosebank area (Passey and Hitchen 2011; Hardman *et al.* 2018).

Biostratigraphic interpretation of two Rosebank wells (exploration well 213/27-3Z and appraisal well 213/27-2: Fig. 1b) was also used to correlate Colsay Member units (1–4) 21.3 km northwards along the central-northern Corona Ridge from the Rosebank Field (213/27-2 and 213/27-3Z) to those we have identified within 213/23-1 (Eriboll) (Fig. 11). To allow a comparison of Colsay Member units, descriptions of the Colsay Member (sequence T40–T45) sandstone units (1–4) from within the Rosebank Field are provided in Table 2, alongside observations of the Colsay intervals we interpret within 213/23-1 (Eriboll).

The two main reservoirs of the Rosebank Field, the Colsay 1 unit and Colsay 3 unit, thin into 213/23-1 (Eriboll) from 213/27-3Z and contain more net claystone. However, the Colsay 2 unit and Colsay 4 units both thicken into 213/23-1 (Eriboll) from Rosebank and contain more net sandstone. Specifically, within 213/23-1, the Colsay 4 unit contains a 25 m-thick sandstone that contains oil shows. Colsay 4 is an interval characterized typically by volcaniclastic siltstones and claystones within the Rosebank Field (Fig. 11). The transition of T45 upper Colsay 1 unit palaeoenvironments from fully marine in Rosebank to shallow-marine shelf in 213/23-1 (Eriboll) (Table 2) supports interpretations of a palaeocoastline by Hardman *et al.* (2018) between Rosebank and 213/23-1 during the deposition of the T45 Colsay 1 interval (post-volcanic rocks).

Log signatures of the four volcanic intervals (Fig. 10) we interpret within the Colsay Member section of 213/23-1 (Eriboll) are not representative, as suggested within the composite log ('intrusive volcanics': Mobil North Sea Ltd 1998), of igneous intrusions encountered within the FSB as described by Mark *et al.* (2018*b*, p. 741, fig. 6). Instead, the intervals have comparable log characteristics with lavas present across the FSB as described by Nelson *et al.* (2009) and Watson *et al.* (2017), and are reinterpreted as such by this study (Fig. 10). The four intervals of volcanic rocks we interpret within 213/23-1 (Eriboll) are also analogous to volcanic image log facies of lava flows from within the Rosebank Field described by Watton *et al.* (2014, pp. 180–182, fig. 6) and Millett *et al.* (2021, p. 2897, fig. 9).

Our reinterpretation of 213/23-1 (Eriboll) has proved the presence of T40–T45 lava flows and possible intra- and sub-basaltic plays north of the Rosebank Field, not previously interpreted this far north (Mobil North Sea Ltd 1999*a*; Passey and Hitchen 2011; Hardman *et al.* 2018). Our results may facilitate further understanding of the true extent and distribution of the intra-basaltic Colsay Member play fairway along the northern Corona Ridge.

Recommendations for future exploration

Many wells along the central-northern Corona Ridge were drilled over 20 years ago (e.g. 213/23-1 Eriboll, 214/09-1 Bunnehaven and 214/04-1 Tobermory: Fig. 1b). Since then, the understanding and subsequent nomenclature of late Paleocene–early Eocene sequences has advanced, which has provided insight into the distribution of Paleogene volcanic rocks (Passey and Hitchen 2011), intra-basaltic lava-field drainage systems (Schofield and Jolley 2013) and lava-field stratigraphy (Passey and Jolley 2009; Hardman *et al.* 2018; Walker *et al.* 2020; Jolley *et al.* 2021).

The results presented in this study emphasize the need for a re-evaluation of wells drilled along the northern Corona Ridge: that is, 214/09-1 (Bunnehaven) and 214/04-1 (Tobermory) (Fig. 1b). Specifically, our results highlight the need for a re-evaluation focused on the possible identification and characterization of Paleocene–Eocene intra- and sub-basaltic Colsay Member sandstone (sequence T40–T45) plays that may have previously been missed (as we demonstrate within 213/23-1, Eriboll). The reinterpretation of wells, integrated with the knowledge gained

from new wells (e.g. Lyon 208/02-1 and Blackrock 204/05b-2: Fig. 1b) and recent publications (e.g. Jolley *et al.* 2021), combined with an appreciation of the complexities of sediment–lava interaction, could not only assist with further locations of sequence T40–T45 intra- and sub-basaltic sand fairways but may also facilitate the development of complex reservoirs such as the Rosebank Field. This approach could provide a strategic method to identifying Paleocene–Eocene targets within the underexplored gas-prone area of the northern FSB, an area that (as of September 2022) holds *c*. 656 bcf of stranded gas as a potential tieback option for any nearby commercial discoveries (post-drill in-place volume estimates: Tobermory 464 bcf, ExxonMobil 2000; Bunnehaven 192 bcf, ExxonMobil 2001).

Conclusions

The Faroe–Shetland Basin is one of the only remaining exploration frontiers on the UK Continental Shelf and will also arguably be one of the most important areas to contribute to indigenous oil and gas supply during the next 40 years. Particularly prospective areas of the FSB include the Rona Ridge and Corona Ridge, intra-basinal highs along which the Clair Field (Rona Ridge), Rosebank Field and Cambo Field (Corona Ridge) have been discovered. Exploration and research have largely focused on both the Rona Ridge and post-rift Paleocene–Eocene-aged prospectivity along the southern Corona Ridge. Whilst hydrocarbon shows and discoveries prove that a working petroleum system is at play within the sub-basins bound by the central-northern Corona Ridge, many aspects of the region's geology are still not fully understood.

Through the interpretation of 3D seismic data integrated with an analysis of three exploration wells (213/23-1 Eriboll, 214/21a-2 South Uist and 213/25c-1V North Uist) we have revealed new insights into the structural configuration, geology and hydrocarbon prospectivity of the central-northern Corona Ridge. We show that:

- The Rosebank intra- and sub-basaltic play concept extends to the NE of the Rosebank Field, along the central-northern Corona Ridge, at least into well 213/23-1 (Eriboll).
- Based on a re-evaluation of available well data, we suggest that Triassic strata are absent along the Corona Ridge, challenging the previous understanding of Triassic distribution within the central Faroe–Shetland Basin. This interpretation also possibly opens further Devonian–Carboniferous-aged exploration plays of the Clair Group (previously interpreted as Triassic) and the possible presence of gas-prone Carboniferous coals within the northern Faroe–Shetland Basin.
- Using 3D seismic data, we present detailed time–structure maps of the northern-central Corona Ridge. Our results show that the structural configuration of the central-northern Corona Ridge is far more complex than previously understood, including north–south- and NNW–SSE-striking faulting oblique to the basinal NE–SW-striking structural trends within the Faroe–Shetland Basin.

Acknowledgements This paper forms part of the lead author's Ph.D. research conducted as part of the Natural Environment Research Council (NERC) Centre for Doctoral Training (CDT) in Oil and Gas at the University of Aberdeen. It is funded by the University of Aberdeen and sponsored by Total E&P UK Ltd, whose support is gratefully acknowledged. PGS are thanked for the generous provision of the FSB MegaSurveyPlus seismic dataset to the PhD project and also for permission to publish part of the dataset (Fig. 3). This paper contains information provided by the North Sea Transition Authority and/or other third parties. Core photographs were obtained from the BGS Offshore well database. Seismic interpretation was undertaken using Schlumberger Petrel software and well-log interpretation was performed using Schlumberger Techlog software, for which the academic licences were kindly provided by Schlumberger and are gratefully acknowledged. Thanks to Conrado Climent, Ole-Petter Hansen, Michael Hertle, Anders Madsen and Stuart Archer for invaluable discussions during the lead author's time spent working with TotalEnergies in Copenhagen. Thanks also to Christopher Bugg and Matthew Rowlands at TotalEnergies in Aberdeen. Reviewers Tony Doré, Peter Dromgoole and Clayton Grove are thanked for their detailed constructive reviews that improved this manuscript. The views held within this paper do not necessarily represent the views of Schlumberger, TotalEnergies and Ørsted.

Author contributions **LKL**: conceptualization (lead), data curation (supporting), formal analysis (lead), investigation (lead), methodology (lead), visualization (lead), writing – original draft (lead), writing – review & editing (lead); **NS**: conceptualization (supporting), data curation (supporting), supervision (supporting), visualization (supporting), writing – original draft (supporting), writing – review & editing (supporting); **DWJ**: conceptualization (supporting), data curation (supporting), visualization (supporting), writing – review & editing (supporting); **SPH**: writing – original draft (supporting); **T-RV**: data curation (supporting), writing – review & editing (supporting); **BAK**: visualization (supporting), writing – review & editing (supporting); **DKM**: writing – review & editing (supporting); **HC**: writing – review & editing (supporting).

Funding The University of Aberdeen (grant No. RT10121-14), Natural Environment Research Council Centre for Doctoral Training (CDT) in Oil and Gas (grant No. NE/M00578X/1). The principal award recipient was L.K. Layfield. Funding was also received by Total E&P UK Ltd (principal award recipient was N. Schofield).

Competing interests The authors declare that they have no known competing financial interests or personal relationships that could have appeared to influence the work reported in this paper.

Data availability The main data that support the findings of this study (Corona 3D, NSTA NDR survey names: TT133D0003 and TT153D0002) are available from the North Sea Transition Authority NDR (https://ndr.nstauthority.co.uk/). Restrictions apply to availability of the PGS FSB MegaSurveyPlus (Fig. 3), which were used under licence for the current study, and so are not publicly available. Well data used throughout this paper are freely available and can be downloaded from the UK NSTA NDR portal. Core photographs were obtained from the BGS Offshore well database.

References

Abdelmalak, M.M., Faleide, J.I., Planke, S., Gernigon, L., Zastrozhnov, D., Shephard, G.E. and Myklebust, R. 2017. The T-reflection and the deep crustal structure of the vøring margin, offshore mid-Norway. *Tectonics*, **36**, 2497–2523, https://doi.org/10.1002/2017TC004617

Austin, J.A., Cannon, S.J.C. and Ellis, D. 2014. Hydrocarbon exploration and exploitation West of Shetlands. *Geological Society, London, Special Publications*, **397**, 1–10, https://doi.org/10.1144/SP397.13

Barr, D., Savory, K.E., Fowler, S.R., Arman, K. and McGarrity, J.P. 2007. Pre-development fracture modelling in the Clair field, west of Shetland. *Geological Society, London, Special Publications*, **270**, 205–225, https://doi.org/10.1144/GSL.SP.2007.270.01.14

Bell, B.R. and Jolley, D.W. 1997. Application of palynological data to the chronology of the Palaeogene lava fields of the British Province: implications for magmatic stratigraphy. *Journal of the Geological Society, London*, **154**, 701–708, https://doi.org/10.1144/gsjgs.154.4.0701

Bonter, D.A. and Trice, R. 2019. An integrated approach for fractured basement characterization: the Lancaster Field, a case study in the UK. *Petroleum Geoscience*, **25**, 400–414, https://doi.org/10.1144/petgeo2018-152

BP Exploration Operating Company Ltd 2013*a*. *213/25c-1V (North Uist) Composite Log*. North Sea Transition Authority UK National Data Repository, File ID: 235670321, https://ndr.nstauthority.co.uk/

BP Exploration Operating Company Ltd 2013*b*. *End of Well Report, 213/25c-1, 1Z, 1Y, 1X, 1W, 1V*. North Sea Transition Authority UK National Data Repository, File ID: 235651767, https://ndr.nstauthority.co.uk/

BP Exploration Operating Company Ltd 2013*c*. *North Uist Exploration Well, 213/25c-1, 1Z, 1Y, 1X, 1W, 1V*. Geological Operations Report. North Sea Transition Authority UK National Data Repository, File ID: 235670049, https://ndr.nstauthority.co.uk/

British Geological Survey 1996. *Tectonic Map of Britain, Ireland and Adjacent Areas (1:500 000)*. Pharaoh, T.C., Morris, J.H., Long, C.B. and Ryan, P.D. (compilers). British Geological Survey, Keyworth, Nottingham, UK, https://largeimages.bgs.ac.uk/iip/mapsportal.html?id=1004599

British Geological Survey 2021. Offshore Hydrocarbon Wells. British Geological Survey, Keyworth, Nottingham, UK, webapps.bgs.ac.uk/data/offshoreWells

ChevronTexaco Upstream Europe 2004. *Rosebank-Lochnagar Exploration Well. 213/27-1 & 1Z End of Well Report. Geological End of Well Report and Lessons Learned*. North Sea Transition Authority UK National Data Repository, File ID: 1968914, https://ndr.nstauthority.co.uk/

Chevron Upstream Europe 2007*a*. *Rosebank / Lochnagar Appraisal Well. Well 213/27-2. Geological End of Well Report and Lessons Learned*. North Sea Transition Authority UK National Data Repository, File ID: 7918905, https://ndr.nstauthority.co.uk/

Chevron Upstream Europe 2007*b*. *Rosebank Appraisal Well. Well 213/26-1*. North Sea Transition Authority UK National Data Repository, File ID: 1936692, https://ndr.nstauthority.co.uk/

Chevron Upstream Europe 2009. *213/27-3 and 3Z. Rosebank–Lochnagar Exploration Well. Geological and Geophysical End of Well Report*. North Sea Transition Authority UK National Data Repository, File ID: 165067809, https://ndr.nstauthority.co.uk/

Clark, J., Mazzuchelli, D., Rowlands, M., Jebara, N. and Parry, C. 2020. The Edradour Field, Block 206/4a, UK Atlantic Margin. *Geological Society, London, Memoirs*, **52**, 952–957, https://doi.org/10.1144/M52-2018-23

CNOOC Ltd 2017. *License P.1192 Relinquishment Report*. North Sea Transition Authority UK National Data Repository, https://www.nstauthority.co.uk/data-centre/nsta-open-data/relinquishments/

Cohen, K.M., Finney, S.C., Gibbard, P.L. and Fan, J.-X. 2013. The ICS international chronostratigraphic chart. *Episodes*, **36**, 199–204, https://doi.org/10.18814/epiiugs/2013/v36i3/002

Conoco (UK) Ltd 1996. *206/5-2 Final Geological Report*. North Sea Transition Authority UK National Data Repository, File ID: 1680196, https://ndr.nstauthority.co.uk/

Coward, M.P. 1990. The Precambrian, Caledonian and Variscan framework to NW Europe. *Geological Society, London, Special Publications*, **55**, 1–34, https://doi.org/10.1144/GSL.SP.1990.055.01.01

Dean, K., McLachlan, K. and Chambers, A. 1999. Rifting and the development of the Faroe–Shetland Basin. *Geological Society, London, Petroleum Geology Conference Series*, **5**, 947–956, https://doi.org/10.1144/0050533

Doré, A.G., Lundin, E.R., Fichler, C. and Olesen, O. 1997. Patterns of basement structure and reactivation along the NE Atlantic margin. *Journal of the Geological Society, London*, **154**, 85–92, https://doi.org/10.1144/gsjgs.154.1.0085

Doré, A.G., Lundin, E.R., Jensen, L.N., Birkeland, Ø., Eliassen, P.E. and Fichler, C. 1999. Principal tectonic events in the evolution of the northwest European Atlantic margin. *Geological Society, London, Petroleum Geology Conference Series*, **5**, 41–61, https://doi.org/10.1144/0050041

Doré, A.G., Lundin, E.R., Kusznir, N.J. and Pascal, C. 2008. Potential mechanisms for the genesis of Cenozoic domal structures on the NE Atlantic margin: pros, cons and some new ideas. *Geological Society, London, Special Publications*, **306**, 1–26, https://doi.org/10.1144/SP306.1

Duncan, L., Helland-Hansen, D. and Dennehy, C. 2009. The Rosebank Discovery, A new play type in intra basalt reservoirs of the North Atlantic volcanic province. *In:* 6th European Production and Development Conference and Exhibition (DEVEX), Abstracts, 13 May, Aberdeen. Chevron Upstream Europe, http://docplayer.net/40657397-The-rosebank-discovery-a-new-play-type-in-intra-basalt-reservoirs-of-the-north-atlantic-volcanic-province-devex-aecc-13-may-2009.html

Duncan, L.J., Dennehy, C.J., Ablard, P.M. and Wallis, D.W. 2020. The Rosebank Field, Blocks 213/27a, 213/26b, 205/1a and 205/2a, UK Atlantic Margin. *Geological Society, London, Memoirs*, **52**, 980–989, https://doi.org/10.1144/M52-2018-42

Ebdon, C.C., Granger, P.J., Johnson, H.D. and Evans, A.M. 1995. Early Tertiary evolution and stratigraphy of the Faeroe–Shetland Basin: implications for hydrocarbon prospectivity. *Geological Society, London, Special Publications*, **90**, 51–69, https://doi.org/10.1144/GSL.SP.1995.090.01.03

Ellis, D. and Stoker, M.S. 2014. The Faroe–Shetland Basin: a regional perspective from the Paleocene to the present day and its relationship to the opening of the North Atlantic Ocean. *Geological Society, London, Special Publications*, **397**, 11–31, https://doi.org/10.1144/SP397.1

Ellis, D., Passey, S.R., Jolley, D.W. and Bell, B.R. 2009. Transfer zones: the application of new geological information from the Faroe Islands applied to the offshore exploration of intra and sub-basalt strata. *In:*Ziska, H. and Varming, T. (eds) Faroe Islands Exploration Conference: Proceedings of the 2nd Conference. Faroese Society of Sciences and Humanities, Tórshavn, 205–226.

Energy Voice 2012. Oil & Gas: North Uist's price tag to exceed £100m. *Energy Voice*, 19 September, https://www.energyvoice.com/oilandgas/29442/north-uists-price-tag-to-exceed-100m/

ExxonMobil 2000. *Well 214/04-1, Post-Drill Report*. North Sea Transition Authority UK National Data Repository, File ID: 244037442, https://ndr.nstauthority.co.uk/

ExxonMobil 2001. *Post-Drill Well Summary Report, Well 214/09-1, Tranche 61*. North Sea Transition Authority UK National Data Repository, File ID: 1807261, https://ndr.nstauthority.co.uk/

Fletcher, R., Kusznir, K., Roberts, A. and Hunsdale, R. 2013. The formation of a failed continental breakup basin: The Cenozoic development of the Faroe–Shetland Basin. *Basin Research*, **25**, 1–22, https://doi.org/10.1111/bre.12015

Funck, T., Geissler, W.H., Kimbell, G.S., Gradmann, S., Erlendsson, Ö., McDermott, K. and Petersen, U.K. 2017. Moho and basement depth in the NE Atlantic Ocean based on seismic refraction data and receiver functions. *Geological Society, London, Special Publications*, **447**, 207–231, https://doi.org/10.1144/SP447.1

Gardiner, D., Schofield, N. *et al.* 2019. Modeling petroleum expulsion in sedimentary basins: the importance of igneous intrusion timing and basement composition. *Geology*, **47**, 904–908, https://doi.org/10.1130/G46578.1

Goodchild, M.W., Henry, K.L., Hinkley, R.J. and Imbus, S.W. 1999. The Victory gas field, West of Shetland. *Geological Society, London, Petroleum Geology Conference Series*, **5**, 713–724, https://doi.org/10.1144/0050713

Hardman, J., Schofield, N., Jolley, D., Hartley, A., Holford, S. and Watson, D. 2018. Controls on the distribution of volcanism and intra-basaltic sediments in the Cambo-Rosebank region, West of Shetland. *Petroleum Geoscience*, **25**, 71–89, https://doi.org/10.1144/petgeo2017-061

Hardwick, A., Travis, T., Stokes, S. and Hart, M. 2010. Lows and highs: using low frequencies and improved velocity tools to image complex ridges and basement highs in the Faroe–Shetland Basin. *First Break*, **28**, 61–67, https://doi.org/10.3997/1365-2397.28.9.41392

Herries, R., Poddubiuk, R. and Wilcockson, P. 1999. Solan, Strathmore and the back basin play, West of Shetland. *Geological Society, London, Petroleum Geology Conference Series*, **5**, 693–712, https://doi.org/10.1144/0050693

Hillis, R.R. 1997. Does the in situ stress field control the orientation of open natural fractures in sub-surface reservoirs? *Exploration Geophysics*, **1–2**, 80–87, https://doi.org/10.1071/EG997080

Hitchen, K. and Ritchie, J.D. 1987. Geological review of the West Shetland area. *In:* Brooks, J. and Glennie, K.W. (eds) *Petroleum Geology of North West Europe*. Graham & Trotman, London, 737–749.

Holdsworth, R.E., Morton, A. *et al.* 2019. The nature and significance of the Faroe–Shetland Terrace: linking Archaean basement blocks across the North Atlantic. *Precambrian Research*, **321**, 154–171, https://doi.org/10.1016/j.precamres.2018.12.004

Holford, S.P., Tassone, D.R., Stoker, M.S. and Hillis, R.R. 2015. Contemporary stress orientations in the Faroe–Shetland region. *Journal of the Geological Society, London*, **173**, 142–152, https://doi.org/10.1144/jgs2015-048

Hughes, S., Barton, P.J. and Harrison, D.J. 1997. Characterizing the Mid-Faeroe Ridge using seismic velocity measurements. *Papers on Geomagnetism and Paleomagnetism Marine Geology and Geophysics*, **102**, 7837–7847, https://doi.org/10.1029/96JB03809

Iliffe, J.E., Robertson, A.G., Ward, G.H.F., Wynn, C., Pead, S.D.M. and Cameron, M. 1999. The importance of fluid pressures and migration to the hydrocarbon prospectivity of the Faeroe–Shetland White Zone. *Geological Society, London, Petroleum Geology Conference Series*, **5**, 601–611, https://doi.org/10.1144/0050601

Jolley, D.W. and Bell, B.R. 2002. The evolution of the North Atlantic Igneous Province and the opening of the NE Atlantic rift. *Geological Society, London, Special Publications*, **197**, 1–13, https://doi.org/10.1144/GSL.SP.2002.197.01.01

Jolley, D.W., Millett, J.M., Schofield, N., Broadley, L. and Hole, M.J. 2021. Stratigraphy of volcanic rock successions of the North Atlantic rifted margin: the offshore record of the Faroe Shetland and Rockall basins. *Earth and Environmental Science Transactions of the Royal Society of Edinburgh*,**112**, 61–88, https://doi.org/10.1017/S1755691021000037

Joseph, S., Lu, X., Bykov, K. and Douillard, A. 2017. Extensive broadband 3D seismic to De-risk and Mature the West of Shetland Exploration Portfolio. *In*: *79th EAGE Conference & Exhibition, 12–15 June, Paris*. European Association of Geoscientists & Engineers (EAGE), Houten, The Netherlands, https://doi.org/10.3997/2214-4609.201700816

Kinny, P.D., Friend, C.R.L. and Love, G.J. 2005. Proposal for a terrane-based nomenclature for the Lewisian Gneiss Complex of NW Scotland. *Journal of the Geological Society, London*, **162**, 175–186, https://doi.org/10.1144/0016-764903-149

Knott, S.D., Burchell, M.T., Jolley, E.J. and Fraser, A.J. 1993. Mesozoic to Cenozoic plate reconstructions of the North Atlantic and hydrocarbon plays of the Atlantic margins. *Geological Society, London, Petroleum Geology Conference Series*, **4**, 953–974, https://doi.org/10.1144/0040953

Lamers, E. and Carmichael, S.M.M. 1999. The Paleocene deepwater sandstone play West of Shetland. *Geological Society, London, Petroleum Geology Conference Series*, **5**, 645–659, https://doi.org/10.1144/0050645

Larsen, M., Rasmussen, T. and Hjelm, L. 2010. Cretaceous revisited: exploring the syn-rift play of the Faroe–Shetland Basin. *Geological Society, London, Petroleum Geology Conference Series*, **7**, 953–962, https://doi.org/10.1144/0070953

Loizou, N. 2014. Success in exploring for reliable, robust Paleocene traps west of Shetland. *In:* Cannon, S.J.C. and Ellis, D. (eds) *Hydrocarbon Exploration to Exploitation West of Shetlands*. Geological Society, London, Special Publications, **397**, 59–79, https://doi.org/10.1144/SP397.9

Makris, J., Papoulia, I. and Ziska, H. 2009. Crustal structure of the Shetland–Faeroe Basin from long offset seismic data. *In:* Ziska, H. and Varming, T. (eds) Faroe Islands Exploration Conference: Proceedings of the 2nd Conference. Faroese Society of Sciences and Humanities, Tórshavn, 30–42.

Mark, N.J., Schofield, N. *et al.* 2018*a*. Overthickening of sedimentary sequences by igneous intrusions. *Journal of the Geological Society, London*, **176**, 46–60, https://doi.org/10.1144/jgs2018-112

Mark, N.J., Schofield, N. *et al.* 2018*b*. Igneous intrusions in the Faroe Shetland basin and their implications for hydrocarbon exploration; new insights from well and seismic data. *Marine and Petroleum Geology*, **92**, 733–753, https://doi.org/10.1016/j.marpetgeo.2017.12.005

Millett, J.M., Jerram, D.A. *et al.* 2021. The Rosebank Field, NE Atlantic: volcanic characterisation of an inter-lava hydrocarbon discovery. *Basin Research*, **33**, 2883–2913, https://doi.org/10.1111/bre.12585

Mobil North Sea Ltd 1998. *213/23-1 Composite Well Log*. North Sea Transition Authority UK National Data Repository, File ID: 1787343, https://ndr.nstauthority.co.uk/

Mobil North Sea Ltd 1999*a*. *Final Geological Well Report 213/23-1 Eriboll*. North Sea Transition Authority UK National Data Repository, File ID: 1817906, https://ndr.nstauthority.co.uk/

Mobil North Sea Ltd 1999*b*. *Well: 213/23-1, Biostratigraphy of the Intervals 4398'–6168' and 6650'–14200'*. North Sea Transition Authority UK National Data Repository, File ID: 242925996, https://ndr.nstauthority.co.uk/

Mobil North Sea Ltd 1999*c*. *Sedimentology and Petrography of Well 213/23-1. Report No. 24/98. Compiled by Leppard Sedimentology & Petroclays*. North Sea Transition Authority UK National Data Repository, File ID: 1809512, https://ndr.nstauthority.co.uk/

Mobil North Sea Ltd 1999*d*. *Exploration Well 213/23-1: Structural and sedimentological interpretation of FMI borehole image data*. North Sea Transition Authority UK National Data Repository, File ID: 1809509, https://ndr.nstauthority.co.uk/

Morton, A. and Milne, A. 2012. Heavy mineral stratigraphic analysis on the Clair Field, UK, west of Shetlands: a unique real-time solution for red-bed correlation while drilling. *Petroleum Geoscience*, **18**, 115–128, https://doi.org/10.1144/1354-079311-026

Morton, A., Hallsworth, C., Kunka, J., Laws, E., Payne, S. and Walder, D. 2010. Heavy-mineral stratigraphy of the Clair Group (Devonian–Carboniferous) in the Clair Field, West of Shetland, U.K. *SEPM Special Publications*, **94**, 183–199, https://doi.org/10.2110/sepmsp.094.183

Moy, D.J. and Imber, J. 2009. A critical analysis of the structure and tectonic significance of rift-oblique lineaments ('transfer zones') in the Mesozoic–Cenozoic succession of the Faroe–Shetland Basin, NE Atlantic margin. *Journal of the Geological Society, London*, **166**, 831–844, https://doi.org/10.1144/0016-76492009-010

Mudge, D.C. and Rashid, B. 1987. The geology of the Faeroe Basin area. *In:* Brooks, J. and Glennie, K.W. (eds) *Petroleum Geology of North West Europe*. Graham & Trotman, London, 751–763.

Nelson, C.E., Jerram, D.A. and Hobbs, R.W. 2009. Flood basalt facies from borehole data: implications for prospectivity and volcanology in volcanic rifted margins. *Petroleum Geoscience*, **15**, 313–324, https://doi.org/10.1144/1354-079309-842

Nichols, G.J. 2005. Sedimentary evolution of the Lower Clair Group, Devonian, West of Shetland: climate and sediment supply controls on fluvial, aeolian and lacustrine deposition. *In:* Dore, A.G. and Vining, B.A. (eds) *Petroleum Geology: North-West Europe and Global Perspectives –Proceedings of the 6th Petroleum Geology Conference*. Geological Society, London, Petroleum Geology Conference Series, **6**, 957–967, https://doi.org/10.1144/0060957

North Sea Transition Authority 2019. *UK Oil and Gas: Reserves and Resources*. North Sea Transition Authority, Aberdeen, UK, https://www.nstauthority.co.uk/data-centre/data-downloads-and-publications/reserves-and-resources/

North Sea Transition Authority 2022. *UK National Data Repository*. North Sea Transition Authority, Aberdeen, UK, https://ndr.nstauthority.co.uk/

Ogilvie, S., Barr, D., Roylance, P. and Dorling, M. 2015. Structural geology and well planning in the Clair Field. *Geological Society, London, Special Publications*, **421**, 197–212, https://doi.org/10.1144/SP421.7

OMV 2015. *Relinquishment Report for Licence P1997*. North Sea Transition Authority UK Open Data Site, https://www.nstauthority.co.uk/data-centre/nsta-open-data/relinquishments/

Passey, S. and Hitchen, K. 2011. Cenozoic (igneous). *In:* Ritchie, J.D., Ziska, H., Johnson, H. and Evans, D. (eds) *Geology of the Faroe–Shetland Basin and Adjacent Areas*. British Geological Survey, Keyworth, Nottingham, UK, 209–228, https://pubs.bgs.ac.uk/publications.html?pubID=B06836

Passey, S. and Jolley, D.W. 2009. A revised lithostratigraphic nomenclature for the Palaeogene Faroe Islands Basalt Group, NE Atlantic Ocean. *Earth and Environmental Science Transactions of the Royal Society of Edinburgh*, **99**, 127–158, https://doi.org/10.1017/S1755691009008044

Peacock, D.C.P. and Banks, G.J. 2020. Basement highs: Definitions, characterisation and origins. *Basin Research*, **32**, 1685–1710, https://doi.org/10.1111/bre.12448

Petersen, U.K. and Funck, T. 2017. Review of velocity models in the Faroe–Shetland Channel. *Geological Society, London, Special Publications*, **447**, 357–374, https://doi.org/10.1144/SP447.7

PGS Geophysical 2013. *Acquisition Report. Galloway, West of Shetlands*. North Sea Transition Authority UK National Data Repository, File ID: 260423458, https://ndr.nstauthority.co.uk/

PGS Geophysical 2015. *Acquisition Report. 3D Corona WOS*. North Sea Transition Authority UK National Data Repository, File ID: 258590723, https://ndr.nstauthority.co.uk/

Poppitt, S., Duncan, L.J., Preu, B., Fazzari, F. and Archer, J. 2018. The influence of volcanic rocks on the characterization of Rosebank Field – new insights from ocean-bottom seismic data and geological analogues integrated through interpretation and modelling. *Geological Society, London, Petroleum Geology Conference Series*, **8**, 373–384, https://doi.org/10.1144/PGC8.6

Quinn, M. and Ziska, H. 2011. Permian and Triassic. *In:* Ritchie, J.D., Ziska, H., Johnson, H. and Evans, D. (eds) *Geology of the Faroe–Shetland Basin and Adjacent Areas*. British Geological Survey, Keyworth, Nottingham, UK, 92–102, https://pubs.bgs.ac.uk/publications.html?pubID=B06836

Quinn, M., Varming, T. and Ólavsdottir, J. 2011. Petroleum Geology. *In:* Ritchie, J.D., Ziska, H., Johnson, H. and Evans, D. (eds) *Geology of the Faroe–Shetland Basin and Adjacent Areas*. British Geological Survey, Keyworth, Nottingham, UK, 254–280, https://pubs.bgs.ac.uk/publications.html?pubID=B06836

Ridd, M.F. 1981. Petroleum geology west of the Shetlands. *In:* Illing, L.V. and Hobson, G.D. (eds) *Petroleum Geology of the Continental Shelf of North-West Europe*. Heyden, London, 414–425.

Ridd, M.F. 1983. Aspects of the Tertiary geology of the Faroe–Shetland Channel. *In:* Bott, M.H.P., Saxov, S., Talwani, M. and Thiede, J. (eds) *Structure and Development of the Greenland–Scotland Ridge: New Methods and Concept*. Plenum Press, New York, 91–108.

Rippington, S., Mazur, S. and Warner, J. 2015. The crustal architecture of the Faroe–Shetland Basin: insights from a newly merged gravity and magnetic dataset. *Geological Society, London, Special Publications*, **421**, 169–196, https://doi.org/10.1144/SP421.10

Ritchie, J.D. and Varming, T. 2011. Jurassic. *In:* Ritchie, J.D., Ziska, H., Johnson, H. and Evans, D. (eds) *Geology of the Faroe–Shetland Basin and Adjacent Areas*. British Geological Survey, Keyworth, Nottingham, UK, 103–122, https://pubs.bgs.ac.uk/publications.html?pubID=B06836

Ritchie, J.D., Johnson, H., Quinn, M.F. and Gatliff, R.W. 2008. The effects of Cenozoic compression within the Faroe–Shetland Basin and adjacent areas. *Geological Society, London, Special Publications*, **306**, 121–136, https://doi.org/10.1144/SP306.5

Ritchie, J.D., Ziska, H., Kimbell, G., Quinn, M. and Chadwick, A. 2011. Structure. *In:* Ritchie, J.D., Ziska, H., Johnson, H. and Evans, D. (eds) *Geology of the Faroe–Shetland Basin and Adjacent Areas*. British Geological Survey, Keyworth, Nottingham, UK, 9–70, https://pubs.bgs.ac.uk/publications.html?pubID=B06836

Roberts, A.W., White, R.S. and Christie, P.A.F. 2009. Imaging igneous rocks on the North Atlantic rifted continental margin. *Geophysical Journal International*, **179**, 1024–1038, https://doi.org/10.1111/j.1365-246X.2009.04306.x

Roberts, D.G., Thompson, M., Mitchener, B., Hossack, J., Carmichael, S. and Bjørnseth, H.M. 1999. Palaeozoic to Tertiary rift and basin dynamics: mid-Norway to the Bay of Biscay – a new context for hydrocarbon prospectivity in the deep water frontier. *Geological Society, London, Petroleum Geology Conference Series*, **5**, 7–40, https://doi.org/10.1144/0050007

Robertson, A.G., Ball, M. *et al.* 2020. The Clair Field, Blocks 206/7a, 206/8, 206/9a, 206/12a and 206/13a, UK Atlantic Margin. *Geological Society, London, Memoirs*, **52**, 980–989, https://doi.org/10.1144/M52-2018-76

Rogers, S.F. 2003. Critical stress-related permeability in fractured rocks. *Geological Society, London, Special Publications*, **209**, 7–16, https://doi.org/10.1144/GSL.SP.2003.209.01.02

Rumph, B., Reaves, C.M., Orange, V.G. and Robinson, D.L. 1993. Structuring and transfer zones in the Faroe Basin in a regional tectonic context. *Geological Society, London, Petroleum Geology Conference Series*, **4**, 999–1009, https://doi.org/10.1144/0040999

Schiffer, C., Doré, A.G. *et al.* 2020. Structural inheritance in the North Atlantic. *Earth-Science Reviews*, **206**, 102975, https://doi.org/10.1016/j.earscirev.2019.102975

Schofield, N. and Jolley, D.W. 2013. Development of intra-basaltic lava-field drainage systems within the Faroe–Shetland Basin. *Petroleum Geoscience*, **19**, 273–288, https://doi.org/10.1144/petgeo2012-061

Schofield, N., Holford, S. *et al.* 2017. Regional magma plumbing and emplacement mechanisms of the Faroe-Shetland Sill Complex: implications for magma transport and petroleum systems within sedimentary basins. *Basin Research*, **29**, 41–63, https://doi.org/10.1111/bre.12164

Schofield, N., Holford, S., Edwards, A., Mark, N. and Pugliese, S. 2020. Overpressure transmission through interconnected igneous intrusions. *AAPG Bulletin*, **104**, 285–303, https://doi.org/10.1306/05091918193

Schöpfer, K. and Hinsch, R. 2019. Late Palaeozoic–Mesozoic tectonostratigraphic development of the eastern Faroe–Shetland Basin: new insights from high-resolution 3D seismic and well data. *Marine and Petroleum Geology*, **109**, 494–518, https://doi.org/10.1016/j.marpetgeo.2019.04.007

Scotchman, I.C., Griffith, C.E., Holmes, A.J. and Jones, D.M. 1998. The Jurassic petroleum system north and west of Britain: a geochemical oil-source correlation study. *Organic Geochemistry*, **29**, 671–700, https://doi.org/10.1016/S0146-6380(98)00183-1

Scotchman, I.C., Carr, A.D. and Parnell, J. 2006. Hydrocarbon generation modelling in a multiple rifted and volcanic basin: a case study in the Foinaven Sub-basin, Faroe–Shetland Basin, UK Atlantic margin. *Scottish Journal of Geology*, **42**, 1–19, https://doi.org/10.1144/sjg42010001

Scotchman, I.C., Doré, A.G. and Spencer, A.M. 2016. Petroleum systems and results of exploration on the Atlantic margins of the UK, Faroes & Ireland: what have we learnt? *Geological Society, London, Petroleum Geology Conference Series*, 8, 187–197, https://doi.org/10.1144/PGC8.14

Shell UK Ltd 2010. *South Uist 214/21a-2 End of Well Report*. North Sea Transition Authority UK National Data Repository, File ID: 96075501, https://ndr.nstauthority.co.uk/

Shell UK Ltd 2014. *Relinquishment Report for License P.799 Relinquishment of Block 214/21a*. North Sea Transition Authority UK Open Data Site https://www.nstauthority.co.uk/data-centre/nsta-open-data/relinquishments/

Sheriff, R.E. and Geldart, L.P. 1982. *Exploration Seismology*. Cambridge University Press, Cambridge, UK.

Siccar Point Energy 2020*a*. *Corona Ridge Area*. Siccar Point Energy, Aberdeen, UK, siccarpointenergy.co.uk/our-portfolio/corona-ridge-area

Siccar Point Energy 2020*b*. *Siccar Point Energy Announces Cambo FID Deferral to 2021*. Siccar Point Energy, Aberdeen, UK, siccarpointenergy.co.uk/uploads/20200330_Cambo_FID_FINAL.pdf

Siccar Point Energy 2020*c*. *Geological Operations End of Well Report 208/02-1 (Lyon)*. North Sea Transition Authority UK National Data Repository, File ID: 333926066, https://ndr.nstauthority.co.uk/

Siccar Point Energy 2020*d*. *Relinquishment Report for Licence P.1854*. North Sea Transition Authority UK Open Data Site, https://www.nstauthority.co.uk/data-centre/nsta-open-data/relinquishments/

Smallwood, J.R. 2004. Tertiary inversion in the Faroe–Shetland Channel and the development of major erosional scarps. *Geological Society, London, Memoirs*, **29**, 187–198, https://doi.org/10.1144/GSL.MEM.2004.029.01.18

Smallwood, J.R. and Gill, C.E. 2002. The rise and fall of the Faroe–Shetland Basin: evidence from seismic mapping of the Balder Formation. *Journal of the Geological Society, London*, **159**, 627–630, https://doi.org/10.1144/0016-764902-064

Smallwood, J.R. and Kirk, W.J. 2005. Paleocene exploration in the Faroe–Shetland Channel: disappointments and discoveries. *Geological Society, London, Petroleum Geology Conference Series*, **6**, 977–991, https://doi.org/10.1144/0060977

Smallwood, J.R. and Maresh, J. 2002. The properties, morphology and distribution of igneous sills: modelling, borehole data and 3D seismic data from the Faeroe–Shetland area. *Geological Society, London, Special Publications*, **197**, 271–306, https://doi.org/10.1144/GSL.SP.2002.197.01.11

Smith, K. and Ziska, H. 2011. Devonian and Carboniferous. *In:* Ritchie, J.D., Ziska, H., Johnson, H. and Evans, D. (eds) *Geology of the Faroe–Shetland Basin and Adjacent Areas*. British Geological Survey, Keyworth, Nottingham, UK, 79–91, https://pubs.bgs.ac.uk/publications.html?pubID=B06836

Sørensen, A.B. 2003. Cenozoic basin development and stratigraphy of the Faroes area. *Petroleum Geoscience*, **9**, 189–207, https://doi.org/10.1144/1354-079302-508

Stoker, M.S. 2016. Cretaceous tectonostratigraphy of the Faroe–Shetland region. *Scottish Journal of Geology*, **52**, 19–41, https://doi.org/10.1144/sjg2016-004

Stoker, M.S. and Varming, T. 2011. Cenozoic (sedimentary). *In:* Ritchie, J.D., Ziska, H., Johnson, H. and Evans, D. (eds) *Geology of the Faroe–Shetland Basin and Adjacent Areas*. British Geological Survey, Keyworth, Nottingham, UK, 151–208, https://pubs.bgs.ac.uk/publications.html?pubID=B06836

Stoker, M.S. and Ziska, H. 2011. Cretaceous. *In:* Ritchie, J.D., Ziska, H., Johnson, H. and Evans, D. (eds) *Geology of the Faroe–Shetland Basin and Adjacent Areas*. British Geological Survey, Keyworth, Nottingham, UK, 123–150, https://pubs.bgs.ac.uk/publications.html?pubID=B06836

Stoker, M.S., Hitchen, K. and Graham, C.C. 1993. *United Kingdom Offshore Regional Report: The Geology of the Hebrides and West Shetland Shelves, and Adjacent Deep-Water Areas*. HMSO for the British Geological Survey, London, https://pubs.bgs.ac.uk/publications.html?pubID=B01843

Stoker, M., Smith, K., Varming, T., Johnson, H. and Olavsdottir, J. 2012. *Eocene (Stronsay Group) Post-Rift Stratigraphy of the Faroe–Shetland Region*. British Geological Survey, Edinburgh, UK, http://nora.nerc.ac.uk/id/eprint/530667/1/CR12009N.pdf

Stoker, M., Doornenbal, H., Hopper, J.R. and Gaina, C. 2014. Tectonostratigraphy. *In:* Hopper, J.R., Funck, T., Stoker, M., Árting, U., Peron-Pinvidic, G., Doornenbal, H. and Gaina, C. (eds) *Tectonostratigraphic Atlas of the North-East Atlantic Region*. Geological Survey of Denmark and Greenland, Copenhagen, 129–212.

Stoker, M.S., Holford, S.P. and Hillis, R.R. 2017*a*. A rift-to-drift record of vertical crustal motions in the Faroe–Shetland Basin, NW European margin: establishing constraints on NE Atlantic evolution. *Journal of the Geological Society, London*, **175**, 263–274, https://doi.org/10.1144/jgs2017-076

Stoker, M.S., Stewart, M.A. *et al.* 2017*b*. An overview of the Upper Palaeozoic–Mesozoic stratigraphy of the NE Atlantic region. *Geological Society, London, Special Publications*, **447**, 11–68, https://doi.org/10.1144/SP447.2

Štolfová, K., and Shannon, P.M. 2009. Permo-Triassic development from Ireland to Norway: basin architecture and regional controls. *Geological Journal Special Issue*, **44**(6), 652–676, https://doi.org/10.1002/gj.1187

Swiecicki, T., Wilcockson, P., Canham, A., Whelan, G. and Homann, H. 1995. Dating, correlation and stratigraphy of the Triassic sediments in the West Shetlands area. *Geological Society, London, Special Publications*, **91**, 57–85, https://doi.org/10.1144/GSL.SP.1995.091.01.04

Tassone, D.R., Holford, S.P., King, R., Tingay, M.R.P. and Hillis, R. 2017. Contemporary stress and neotectonics in the Otway Basin, southeastern Australia. *Geological Society, London, Special Publications*, **458**, 49–88, https://doi.org/10.1144/SP458.10

The Expro Group 1999. *213/23-1 Well Site Test Report*. North Sea Transition Authority UK National Data Repository, File ID: 218487019, https://ndr.nstauthority.co.uk/

Trice, R. 2014. Basement exploration, West of Shetlands: progress in opening a new play on the UKCS. *Geological Society, London, Special Publications*, **397**, 81–105, https://doi.org/10.1144/SP397.3

Underhill, J.R. 2003. The tectonic and stratigraphic framework of the United Kingdom's oil and gas fields. *Geological Society, London, Memoirs*, **20**, 17–59, https://doi.org/10.1144/GSL.MEM.2003.020.01.04

Walker, F., Schofield, N., Millett, J., Jolley, D., Hole, M. and Stewart, M. 2020. Paleogene volcanic rocks in the northern Faroe–Shetland Basin and Møre Marginal High: understanding lava field stratigraphy. *Geological Society, London, Special Publications*, **495**, https://doi.org/10.1144/SP495-2019-13

Watson, D., Schofield, N. *et al.* 2017. Stratigraphic overview of Palaeogene tuffs in the Faroe–Shetland Basin, NE Atlantic Margin. *Journal of the Geological Society, London*, **174**, 627–645, https://doi.org/10.1144/jgs2016-132

Watson, D., Schofield, N., Maguire, A., Telford, C., Mark, N., Archer, S. and Hardman, J. 2019. Raiders of the Lost Mud: the geology behind drilling incidents within the Balder Formation around the Corona Ridge, West of Shetland. *Petroleum Geoscience*, **26**, 110–125, https://doi.org/10.1144/petgeo2018-060

Watton, T.J., Cannon, S., Brown, R.J., Jerram, D.A. and Waichel, B.A. 2014. Using formation micro-imaging, wireline logs and onshore analogues to distinguish volcanic lithofacies in boreholes: examples from Palaeogene successions in the Faroe–Shetland Basin, NE Atlantic. *Geological Society, London, Special Publications*, **397**, 173–192, https://doi.org/10.1144/SP397.7

White, R.S., Spitzer, R., Christie, P.A.F., Roberts, A., Lunnon, Z., Maresh, J. and iSIMM Working Group 2005. Seismic imaging through basalt flows on the Faroes Shelf. *In:* Ziska, H., Varming, T. and Blotch, D. (eds) Faroe Islands Exploration Conference: Proceedings of the 1st Conference. Faroese Society of Sciences and Humanities, Tórshavn, 11–31.

White, R.S., Smith, L.K., Roberts, A.W., Christie, P.A.F., Kusznir, N. and the iSimm Team 2008. Lower-crustal intrusion on the north Atlantic continental margin. *Nature*, **452**, 460–464, https://doi.org/10.1038/nature06687

Wrona, T., Magee, C., Fossen, H., Gawthorpe, R.L., Bell, R.E., Jackson, C.A.-L. and Faleide, J.I. 2019. 3-D seismic images of an extensive igneous sill in the lower crust. *Geology*, **47**, 729–733, https://doi.org/10.1130/G46150.1

Ziska, H. and Anderson, C. 2005. Exploration opportunities in the Faroe Islands. *In:* Ziska, H., Varming, T. and Blotch, D. (eds) Faroe Islands Exploration Conference: Proceedings of the 1st Conference. Faroese Society of Sciences and Humanities, Tórshavn, 146–162.

Ziska, H. and Varming, T. 2008. Palaeogene evolution of the Ymir and Wyville Thomson ridges, European North Atlantic margin. *Geological Society, London, Special Publications*, **447**, 357–374, https://doi.org/10.1144/SP447.7